

AD-A163 954

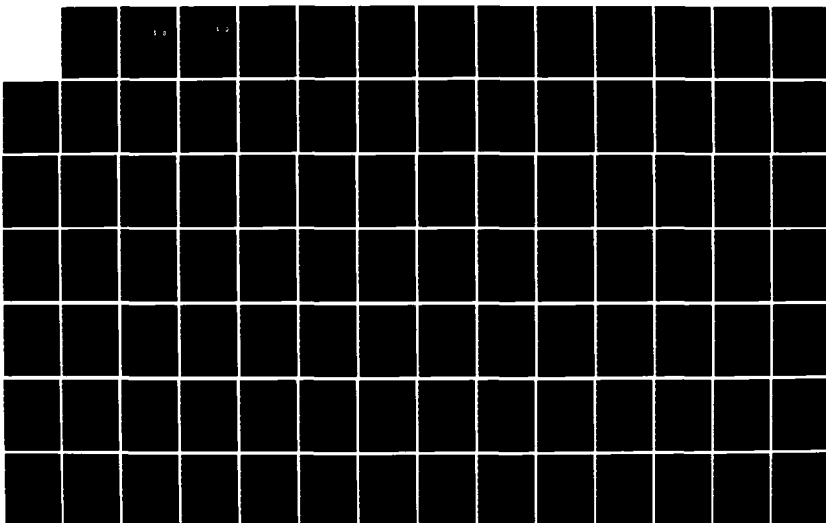
LASER COOLING OF NEUTRAL ATOMS(U) AIR FORCE INST OF  
TECH WRIGHT-PATTERSON AFB OH SCHOOL OF ENGINEERING  
M G NCHARG DEC 83 AFIT/GEP/PH/83D-6

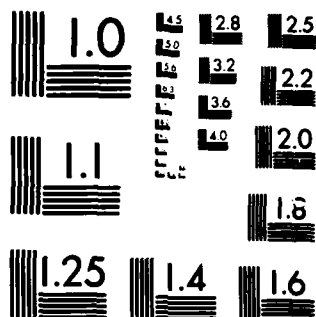
1/2

UNCLASSIFIED

F/G 20/8

NL





MICROCOPY RESOLUTION TEST CHART  
NATIONAL BUREAU OF STANDARDS 1963-A

AD-A163 954



DTIC  
ELECTE  
FEB 13 1986

S  
D

NEUTRAL ATOMS

THESIS

Matthew G. McHarg  
First Lieutenant, USAF

AFIT/GEP/PH/83D-6

**DISTRIBUTION STATEMENT A**

Approved for public release;  
Distribution Unlimited

DEPARTMENT OF THE AIR FORCE  
AIR UNIVERSITY

**AIR FORCE INSTITUTE OF TECHNOLOGY**

Wright-Patterson Air Force Base, Ohio

DTIC FILE COPY

96 2 1 0 016

1

DTIC  
ELECTE  
FEB 13 1988  
S D

LASER COOLING OF  
NEUTRAL ATOMS

THESIS

Matthew G. McHarg  
First Lieutenant, USAF

AFIT/GEP/PH/83D-6

AFIT/GEP/PH/83D-6

LASER COOLING OF  
NEUTRAL ATOMS

THESIS

Presented to the Faculty of the School of Engineering  
of the Air Force Institute of Technology

Air University

In Partial Fulfillment of the  
Requirements for the Degree of  
Master of Science

by

Matthew G. McHarg, B.S.

First Lieutenant, USAF

Graduate Engineering Physics

December 1983



Accession For	
NTIS CRA&I	<input checked="checked" type="checkbox"/>
DTIC TAB	<input type="checkbox"/>
Unannounced	<input type="checkbox"/>
Justification	
By	
Distribution/	
Availability Codes	
Dist	Avail and/or Special
A-1	

Approved for public release; distribution unlimited.

## Acknowledgements

I would like to thank Dr. Richard Cook for his guidance and critical judgement. Dr. Cook developed the theory used in this thesis, and first perceived the need for this thesis to be accomplished. His judgement and clear thinking made this thesis possible. I would also like to acknowledge the master skills of my good friend Julius T. Bear who labored many hours typing this thesis. Finally, I would like to thank my wife, Sabrina Mc Harg. Without her love and support this thesis would not have been completed.

Matthew G. Mc Harg

## Table of Contents

	Page
Acknowledgements .....	ii
List of Figures .....	iv
List of Tables .....	v
Abstract .....	vi
I. Introduction .....	1
Background .....	1
Problem Statement .....	2
Current Knowledge .....	3
Approach .....	3
Assumptions and Scope .....	4
II. Theory of the Resonance Radiation Force .....	7
Introduction .....	7
General Explanation .....	7
Specific Explanation .....	8
The Optical Bloch Equations .....	13
The Fokker-Planck Equation .....	14
Discussion .....	23
III. Application of the Theory to Cooling an Atomic Beam	26
Introduction .....	26
The Fokker-Planck Equation as a Difference	
Equation .....	26
Slowing an Atomic Beam Using a	
Scanning Frequency Laser .....	31
Stability and Convergence Analysis .....	35
Analysis of Scanning Frequency Laser Cooling ...	49
Discussion .....	72
IV. Conclusions and Recommendations .....	86
Review of Major Results .....	86
Conclusions .....	88
Recommendations .....	89
Bibliography .....	91
Appendix .....	94
Vita .....	107

## List of Figures

Figure	Page
1. Flowchart for FPLK Program .....	52
2. Initial Distribution .....	57
3. Distribution With No Frequency Scan .....	58
4. Initial Distribution for 480 MHz Scan .....	61
5. Final Distribution for 480 MHz Scan .....	62
6. Initial Distribution for 750 MHz Scan .....	64
7. Final Distribution for 750 MHz Scan .....	65
8. Initial Distribution for Maximum Cooling Scan .....	66
9. Second Distribution for Maximum Cooling Scan .....	67
10. Third Distribution for Maximum Cooling Scan .....	68
11. Fourth Distribution for Maximum Cooling Scan .....	69
12. Fifth Distribution for Maximum Cooling Scan .....	70
13. Final Distribution for Maximum Cooling Scan .....	71
14. Prodan and Phillips Experimental Data (Ref 10: 139)	75
15. Initial Distribution for 480 MHz Accelerated Scan .	77
16. Final Distribution for 480 MHz Accelerated Scan ...	78
17. Data Input Format for FPLK Program .....	95
18. Data Output Format for FPLK Program .....	97
19. Graphics Program .....	99
20. Plotting Program .....	101



## List of Tables

Table	Page
I. Comparison of vs For Method 1 Stability and Convergence Requirements .....	50
II. Comparison of Experimental, Numerical, and Theoretical Values For Swept Frequency Laser Cooling .....	73
III. Effect of Halving Velocity Increment on Numerical Results .....	83

Abstract

The theory of the resonance radiation force is studied as it applies to the slowing of a two-level atom using a swept frequency laser. The theory is developed in detail for this case. A single partial differential equation called the Fokker-Planck equation is found to describe the atomic motion for many cases. This equation is solved numerically for a one dimensional geometry. Results from this numerical solution are found to be within 10% of experimental results. Analysis of this problem in one dimension leads to the prediction that for fixed amounts of frequency sweeping, a faster scan rate will yield smaller full width at half maximum (FWHM) spread in the velocity distribution for the atomic beam. This program also predicts that the atoms can be slowed arbitrarily close to 0 m/sec using this technique. The program used for this analysis is included.

# LASER COOLING OF NEUTRAL ATOMS

## I. Introduction

### Background

The theory of interaction of light with neutral atoms was first developed by Einstein (Ref 1) in 1917. In this paper Einstein introduced the concept of coefficients that describe absorption, spontaneous and stimulated emission. He described how these coefficients allow derivation of the Planck radiation law and developed the theory of motion of atoms when interacting with light. The momentum transferred to the atoms, and the fluctuations in this transferred momentum, were calculated using quantized energy theory and the idea of the canonical distribution of states in thermal radiation. The first experimental work showing transfer of momentum to an atomic beam was performed by Frisch (Ref 2). Using conventional light sources, Frisch deflected an atomic beam. The advent of the laser, with high intensities and monochromatic nature, greatly enhanced the experimental worlds ability to slow atoms using light.

In 1975 Hansch and Schawlow (Ref 3) first proposed that a standing wave laser could slow atoms using the spontaneous force. Very slow  $< 10$  m/sec atomic beams are useful for atomic clocks (Ref 4 and 5), doppler free spectroscopy (Ref 6), and insertion into single atom light traps (Ref 7).

In 1979 Balykin, Letokhov, and Minogin reported experimentally slowing atoms using a traveling wave constant frequency laser to slow atoms. The reduction in velocity was small, but the distribution functions full width at half maximum (FWHM) was substantially reduced (Ref 8). In 1982 Phillips and Metcalf reported the first observation of slowing using a fixed frequency laser. The difference between the two methods is how the laser stays in resonance with the atomic beam. In the first case the frequency is changed to stay in resonance, and in the second a magnetic field is used to change the energy levels so as to stay in resonance with the laser. In two separate papers (Ref 9 and 10) Phillips and Metcalf, along with Prodan, reported results of the two different methods of cooling. Unfortunately in both cases the laser apparently quit interacting with the atomic beam. In both cases the most probable velocity was 1100 m/sec. In one case the atoms could only be slowed to  $\sim 40$  m/sec. In the second case the atoms were only slowed to  $\sim 600$  m/sec. Consultation between the scientists at National Bureau of Standards and Dr. Richard Cook of the Air Force Institute of Technology resulted in a theoretical investigation of this problem using a one dimensional Fokker-Planck equation. This thesis is the result of that investigation.

### Problem Statement

Given a longitudinal velocity distribution for an atomic beam, and the theory of resonance radiation interacting with that beam, predict the time history of the velocity distribution

using a numerical solution to the Fokker-Planck equation. A careful investigation of the one dimensional model developed by Cook (Ref 11) is to be accomplished. The model will be checked against known experimental results. If the model shows the loss of interaction as found experimentally, then a study of ways to avoid the interaction loss will be undertaken. If the model does not contain the information, other more complex models will be briefly reviewed to find avenues of further research.

### Current Knowledge

The background section gives a historical development of the important papers in this field. Hence, this section will be constrained to dealing with the body of knowledge needed for the thesis. This consists of three basic areas. First, the initial velocity distribution for the atoms are needed. This information is developed in Ramsey's book (Ref 12). Second, a general theory of the interaction of light with an atom is required. A general theory of resonance radiation pressure of light is developed from quantum electrodynamics by Cook (Ref 13). Finally, the transformation of the partial differential equation developed from the theory to a difference equation is taken from Gerald (Ref 14).

### Approach

This thesis is broken into four main sections. The first section is the introduction. The following three sections are the main body of the thesis. A bibliography and an appendix

follow the main portion of the work. The following is a brief description of the main sections in the thesis.

Section II develops a set of coupled differential equations that describe the interaction of the laser with the atomic beam. These equations are developed using Ehrenfests theorem to find the time rate of change of the expectation value of the momentum of the atom. It is shown that these coupled differential equations reduce to a single Fokker-Planck equation in certain circumstances. The Fokker-Planck equation describes the velocity distribution function of the atomic beam as it evolves in time. The Fokker-Planck equation is the major starting point for this thesis.

Section III describes the numerical solution of the Fokker-Planck equation. A difference equation is developed to solve the problem numerically. Stability and convergence criteria of this difference equation are studied. A complete analysis of a particular cooling method is also studied. The results derived from the numerical analysis are compared to experimentally derived results for this particular case.

Section IV draws conclusions and makes recommendations for further work based upon this thesis. A review of the major theory and results are presented in brief form. An estimate of the validity of these results is given. Recommendations are made for further experimental and theoretical work in this area.

#### Assumptions and Scope

Several assumptions are implicit throughout this thesis.

The assumptions are detailed below, along with their justifications, so the reader can gain a clear understanding of the limits of this work. In all cases a minimum number of assumptions are made. Hopefully this will keep the theoretical results broad enough so they can be applied to other specific cases. The theory developed here and elsewhere in the literature assumes that the atom under consideration has only two energy levels. At the present time there are no general solutions to the problem for multi-level atoms. Experimentally, a magnetic field can be applied to the atomic beam to allow only two energy levels to be occupied by the electrons (Ref 15). Thus, the theoretical results can be compared to experimental results without correcting for this assumption.

Only a one dimensional model of the interaction is considered. There are indications that this assumption will cause some results to be ignored in the model that are present in experimental work (Ref 9 pg 1151). This assumption is made since this is the first time that numerical solutions of the Fokker-Planck equation for this situation have been attempted. An inclusion of two and three dimensional effects can be added at a later time to the difference equation. The major result of this assumption is, the finite extent and Gaussian nature of the laser beam is ignored. Since the number density in the atomic beam is very low, approximately  $10^{13} \text{ cm}^{-3}$ , particle-particle interactions in the beam can safely be ignored for a first order answer.

To allow the Fokker-Planck equation to be used as the master equation governing the atomic motion, it is assumed that the external field changes amplitude slowly in time compared to  $\tau = \frac{1}{A}$ . Here  $A$  is the Einstein spontaneous emission coefficient. Since the case considered is a traveling wave monochromatic field interacting with the atomic beam, the above assumption is justified. If the external field is a standing wave, and the atoms are moving with respect to the nodal points, the above assumption would be unwarranted.

The scope of this thesis is intentionally limited due to time constraints. First the theory of resonance radiation is reviewed in the literature and applied to a specific cooling case. Second this specific case is analyzed in detail. Third the theoretical results are compared to experimental results, and are reviewed for possible future options for continuing work in this important area.



## II. Theory of the Resonance Radiation Force

### Introduction

This section contains physical explanation of the interaction of a laser beam in resonance or near resonance conditions with an atomic beam. A qualitative explanation will be given first to provide a general idea of the physics involved in cooling a beam. A quantitative explanation of the physics will follow. The specific explanation is a compilation of several articles by Dr. R.J. Cook (Ref 11 and 13).

### General Explanation

When light interacts with an atom it excites the electrons in the outer shell of the atom to a higher state of energy. In 1917 Einstein (Ref 1) gave the first explanation of this process. Photons have definite momentum and energy described by the famous relations,

$$\vec{P} = \hbar \vec{k} \quad \text{and} \quad E = \hbar \omega$$

where  $\vec{k}$  has magnitude  $\frac{\omega}{c}$  and points in the direction of propagation of the light wave. A photon striking an atom excites the electrons when the energy carried by the photon equals the energy gap between the electronic transitions. When this happens the photon imparts momentum to the atom. After a time where  $\tau = \frac{1}{A}$ ,  $A$  is the Einstein spontaneous emission coefficient, the atom will decay back to the ground state. At this point it can be excited by another photon and receive another "kick" in momentum. If the photons are collimated as in a

laser, the imparted momentum will all be in the same direction. Einstein showed that spontaneous emission has equal probability of emitting in the positive or negative direction for a one dimensional case (Ref 1 pg 67). The emission pattern of the atom while not isotopic, is symmetric. Thus, the spontaneous emission of the atom imparts no net momentum change to the atom. A large number of photon-atom collisions will then cause the beam to be slowed down if the atoms are propagating in the opposite direction of the laser.

### Specific Explanation

Consider an atom with two allowable energy states,  $E_1$  and  $E_2$ . This atom is exposed to a traveling wave tuned to the transition from  $E_1$  to  $E_2$ . This traveling wave has an associated energy density  $W$ . Let  $P_1$  and  $P_2$  be the probability that energy states  $E_1$  or  $E_2$  is occupied. Einstein proposed that in this case the rate of stimulated emission is

$R_{\text{stimulated}} = BWP_2$ . The rate of spontaneous emission is

$R_{\text{spontaneous}} = AP_2$ . Here  $B$  and  $A$  are the Einstein  $B$  and  $A$  coefficients for stimulated and spontaneous emission respectively. For an atom in steady state condition, i.e. the field has been interacting with the atom on a time scale long compared to  $\tau = \frac{1}{A}$ , the rate of exciting processes equal the rate of deexciting process.

Hence,

$$R_{\text{stimulated}} + R_{\text{spontaneous}} = R_{\text{absorbed}}$$

$$\therefore WB(P_2 - P_1) = -AP_2.$$

The atom receives  $+\hbar k$  from the absorption and  $-\hbar k$  from the stimulated emission. So the time rate of change of the momentum is given by equation 1.

$$\bar{F} = \frac{\Delta p}{\Delta t} = \frac{dp}{dt} = -BW(P_2 - P_1)\hbar k = A\hbar P_2 \bar{k} \quad (1)$$

This derivation of the force is accurate only for cases where the momenta transferred has definite value  $\hbar k$ . If the field has a variety of component wavelengths, has  $\bar{k}$ 's pointing in different directions or is not a traveling wave, a more general explanation is required to predict the observed experimental results.

Two papers by Cook (Ref 11 and 13) provide a more general theory of the equations of motion of the atomic beam. The first paper treats the motion of the center of mass of the particle using Ehrenfests theorem and the optical Bloch equations. It neglects fluctuations in the force of the photons on the atoms due to the spontaneous and stimulated emission of the atoms. The second paper develops a general theory for a two level atom in a resonate or near resonate field of arbitrary amplitude and phase. The following will be development of the approach used for Ehrenfests theorem and the optical Bloch equations.

Following Schiff (Ref 15) consider an atom represented by a wave function  $\psi$ . To find the "equation of motion" of this wave packet take the time derivative of the expectation value of the position variable.

$$\frac{d}{dt} \langle x \rangle = \frac{d}{dt} \int \psi^* x \psi d\tau = \int \frac{d\psi^*}{dt} x \psi d\tau + \int \psi^* x \frac{d\psi}{dt} d\tau$$

Substitute for the time derivatives using Schrodingers wave equation and perform some algebra to obtain,

$$\frac{d}{dt} \langle x \rangle = \frac{i\hbar}{2m} \int [ \psi^* x (\nabla^2 \psi) - (\nabla^2 \psi^*) x \psi ] d\tau$$

Integrate over the second term by parts twice remembering that the wave function vanishes at infinity.

$$\frac{d}{dt} \langle x \rangle = \frac{i\hbar}{2m} \int \psi^* [ x \nabla^2 \psi - \nabla^2 (x\psi) ] d\tau$$

Perform the differentiation within the brackets to obtain,

$$\frac{d}{dt} \langle x \rangle = -\frac{i\hbar}{m} \int \psi^* \frac{d\psi}{dx} d\tau = \frac{\langle p \rangle}{m} \quad (2)$$

Using the relation,

$$\langle p \rangle = i\hbar \int \psi^* \frac{d\psi}{dx} d\tau .$$

In a very similar way one can obtain,

$$m \frac{d^2 \langle x \rangle}{dt^2} = \frac{d \langle p \rangle}{dt} = - \left\langle \frac{\partial V}{\partial x} \right\rangle \quad (3)$$

where  $V$  is the potential energy of the system. This is a good representation in the macroscopic limit where the finite size and internal structure of the particle can be ignored. This means the size of the wave packet is small compared to

distance over which  $V$  changes significantly. Equation 1 and 2 provide an analogy to the classical equations of motion. They also agree with the Heisenberg representation which states,

$$\frac{\partial \hat{x}}{\partial t} = \frac{1}{i\hbar} [\hat{x}, \hat{H}] = \nabla_p \hat{H} = \frac{\hat{p}}{m} \quad \text{and,}$$

$$\frac{\partial \hat{p}}{\partial t} = \frac{1}{i\hbar} [\hat{p}, \hat{H}] = -\nabla_R \hat{H} = -\frac{\partial V}{\partial \mathbf{R}} = \nabla_R (\bar{\mu} \cdot \bar{E}).$$

This is because  $-\bar{\mu} \cdot \bar{E}$  is the potential energy for an atom in a field. Here  $\hat{H}$  is the Hamiltonian of the system. For an atom in the dipole approximation of an external field,

$$\hat{H} = \frac{\hat{p}^2}{2m} + \hat{H}_0 - \bar{\mu} \cdot \bar{E}(\bar{R}, t)$$

Here  $\bar{\mu}$  is the electric dipole moment operator and  $\bar{E}$  is the electric field evaluated at a point  $\bar{R}$ .  $\hat{H}_0$  is the Hamiltonian for the internal motion of the atom.

Ehrenfests theorem is equation 4. It is obtained by combining the expectation values of the Heisenberg equations and setting,

$$F = m \frac{d^2 \langle \hat{x} \rangle}{dt^2} = \frac{d\bar{p}}{dt} = \left\langle \nabla_R (\bar{\mu} \cdot \bar{E}) \right\rangle \quad (4)$$

Equation 4 is general as long as the dipole approximation is accepted. To ease calculations, assume that the external field has the form,

$$\vec{E} = \hat{e} E(\vec{r}, t)$$

where  $\hat{e}$  is a polarization vector independent of  $\vec{r}$  and  $t$ . This form of  $\vec{E}$  is substituted into equation 4 to obtain equation 5.

$$\vec{F} = \langle \nabla_R (\vec{\mu} \cdot \vec{E}) \rangle = \langle \vec{\mu} \cdot \hat{e} \rangle \nabla_R E(\vec{r}, t) \quad (5)$$

This uses the assumption that the wave packet is small compared to the changes in the field. This allows the  $\nabla_R E(\vec{r}, t)$  to be pulled out of the expectation value. Therefore in the dipole approximation the motion of the atom is due to the electric field vector. To find the force acting upon the atom, and hence its quantum mechanical "equation of motion", consider a two level atom with energy states  $E$  and  $E$ . An arbitrary monochromatic field is applied to the system. The form of this field is equation 6.

$$E(\vec{r}, t) = \frac{1}{2} E(\vec{r}) \exp \{ i [ \theta(\vec{r}) + \omega t ] \} + \text{complex conjugate} \quad (6)$$

### The Optical Bloch Equations

Several authors (Ref 11 and 16) show that using equation 6 as the applied field in equation 5, yields a coupled set of differential equations. These equations explain the motion of an atom in an external field. Equations 8 thru 10 are the optical Bloch equations. These equations govern the internal workings of these atoms.

$$\vec{F} = m \vec{\ddot{r}} = \frac{1}{2} \hbar (\vec{U} \nabla \Omega + \vec{V} \Omega \nabla \Theta) \quad (7)$$

$$\dot{U} = (\Delta + \dot{\Theta}) V - \frac{1}{2} A U \quad (8)$$

$$\dot{V} = -(\Delta + \dot{\Theta}) U + \Omega W - \frac{1}{2} A U \quad (9)$$

$$\dot{W} = -\Omega V - A(W + 1) \quad (10)$$

Here  $\Theta(\vec{r})$  is the phase of the external field,

$E(\vec{r})$  is the amplitude of that field,

$\Omega = \frac{\mu E}{\hbar}$  is the on resonance Rabi flopping frequency,

$\Delta = \omega - \omega_0$  is the detuning frequency,

$A = \frac{4\omega_0^3}{3\pi c^3} |\langle 1, \mu | 2 \rangle|^2$  is the Einstein spontaneous emission coefficient.

The Rabi frequency is a measure of the field strength at the point under consideration. It also represents the frequency at which the atom will absorb and undergo stimulated emission in a strong field. Equations 7 thru 10 show that the force is not an explicit function of position, velocity, or external field,

but rather is governed by the coupled set of equations shown. The terms involving the Einstein coefficient are called relaxation terms. They are obtained thru quantum electrodynamics and are not derived in this thesis. Louisell (Ref 17) presents a first principles argument for these relaxation terms.

If the spontaneous terms were not present, the atom would oscillate between the upper and lower state at the Rabi frequency. The spontaneous emission process, which gives rise to the relaxation terms, causes a steady state population distribution. The physical significance of the variables  $U, V, W$  are summarized from Allen and Eberly's book (Ref 11).  $W$  is the single atom population inversion,  $V$  is the absorptive component of the dipole moment, and  $U$  is the dispersive component of the dipole moment.

#### The Fokker-Planck Equation

Cook (Ref 13 pg 1087) develops a set of equations similar in nature to equations 7 thru 10. The equations developed by Cook are more general in nature and are derived from quantum electrodynamics. The optical Bloch equations are developed from the Ehrenfests theorem and only predict the equation of motion of the centroid of the atomic wave packet. The optical Bloch equations are consistent with the more general set of equations. It is this fact that allows use of the optical Bloch equations in the development of the theory. The optical Bloch equations represent a less general but still useful starting



point for most practical applications.

An easier way of treating the motion of an atomic beam interacting with a laser is to use the Fokker-Planck equation. Using the general set of equations developed by Cook, it can be shown that the Fokker-Planck equation is accurate to second order in  $\hbar$  (Ref 13 pg 1096). An explicit derivation of the Fokker-Planck equation is given in the Appendix of Cook's paper (Ref 13 pg 1096). The form of the Fokker-Planck equation is given in equation 11.

$$\frac{\partial \xi}{\partial t} = - \frac{\partial}{m \partial v} (F \xi) + \frac{\partial^2}{m^2 \partial v^2} (D \xi) \quad (11)$$

where  $\xi$  is the velocity distribution function for the atomic beam,

$F$  is the interaction force of the laser with the beam,

$m$  is the mass of the atom and

$D$  is a diffusion coefficient.

Since the derivation of the Fokker-Planck equation is given explicitly by Cook, it will not be repeated here. The restrictions imposed by using the equation, and the development of explicit expressions included in the equation are presented below.

The major constraint imposed by the use of the Fokker-Planck equation is the smooth field approximation discussed by Cook (Ref 13 pg 1096). The smooth field approximation requires that the amplitude and phase of the external field remain nearly constant during a time equal to the relaxation time of the atom. This relaxation time is on the order of  $\tau \sim \frac{1}{\Delta}$ .

where  $A$  is the Einstein coefficient. If the amplitude and phase of the external field are not constant in space, then the velocity of the atom must be such that it will not move into a region of significantly different amplitude or phase in a time  $t = \tau$ . For instance, in a standing wave of wavelength  $\lambda$ , the atom should not move a distance greater than  $\frac{\lambda}{v_0}$  during the time  $\tau$ .

The interaction force in equation 11 is derived from equations 7 thru 10. In the case of the smooth field approximation since the phase and amplitude vary slowly in time, the values of  $U, V, W$  assume steady state values obtained by setting  $\dot{U}, \dot{V}, \dot{W} = 0$  in equations 8 thru 10. After elimination of  $W$  one obtains equations 12 thru 14.

$$\vec{F} = \frac{1}{2} \hbar (U \nabla \Omega + V \Omega \nabla \theta) \quad (12)$$

$$U = -4\Omega(\Delta + \dot{\theta}) / [4(\Delta + \dot{\theta})^2 + A^2 + 2\Omega^2] \quad (13)$$

$$V = -2A\Omega / [4(\Delta + \dot{\theta})^2 + A^2 + 2\Omega^2] \quad (14)$$

Solving these three equations for  $F$  results in,

$$\vec{F} = \frac{-[\hbar A \Omega^2 \nabla \theta + \hbar(\Delta + \dot{\theta}) \nabla \Omega^2]}{[4(\Delta + \dot{\theta})^2 + A^2 + 2\Omega^2]} \quad (15)$$

For a plane running wave of the form,

$$\mathcal{E}(\vec{x}, t) = \mathcal{E}_0 \cos(\vec{k} \cdot \vec{x} - \omega t) \quad \Omega = \frac{\mu \mathcal{E}_0}{\hbar} = \text{constant} \quad (16)$$

$$\Theta = -\vec{k} \cdot \vec{x} \Rightarrow \dot{\Theta} = -\vec{k} \cdot \vec{v} \quad \nabla \Theta = -\vec{k} \quad \text{so,}$$

$$\vec{F} = \frac{A \Omega^2 \hbar \vec{k}}{[4(\Delta - \vec{k} \cdot \vec{v})^2 + A^2 + 2\Omega^2]} \quad (17)$$

This is the force associated with the absorption of momenta from photons discussed in the General Explanation section. This force is commonly called the spontaneous emission force since it is the symmetric emission pattern of spontaneous emission, that allows the momenta transferred from absorption to effect the atom.

For a standing wave of the form,

$$\mathcal{E}(\vec{x}, t) = \mathcal{E}(x) \cos(\omega t) \quad \Omega = \frac{\mu \mathcal{E}(x)}{\hbar} \quad \Theta = 0 \quad (18)$$

so that,

$$\vec{F} = \frac{-\hbar \Delta \nabla \Omega^2}{[4\Delta^2 + A^2 + 2\Omega^2]} \quad (19)$$

This force is commonly called the dipole interaction force. This force arises from the dipole moment induced by the external field in the atom interacting with the gradient of the amplitude of the external field. In general, all one needs is the form of the external field. This combined with equation 15 gives the force of interaction between the light

and the atomic beam.

The diffusion coefficient in equation 11 arises because of fluctuations in the interaction force. The diffusion coefficient has two components, one due to the spontaneous emission process, and one due to the induced processes of absorption and stimulated emission. The derivation of the form of the diffusion coefficients is given by Cook (Ref 13 pg 1097). The results of this derivation are equations 20 and 21.

$$D_{ii}^{(s)} = \frac{\hbar^2 A \Omega^2 \hbar^2 d_{ii}^{(s)}}{5(4\Delta_e^2 + A^2 + 2\Omega^2)} \quad (\text{spontaneous}) \quad (20)$$

$$D_{ii}^{(i)} = \alpha \frac{\partial \Omega}{\partial x_i} \frac{\partial \Omega}{\partial x_i} + \beta \Omega^2 \frac{\partial \Theta}{\partial x_i} \frac{\partial \Theta}{\partial x_i} + \gamma \left( \frac{\partial \Omega^2}{\partial x_i} \frac{\partial \Theta}{\partial x_i} + \frac{\partial \Theta}{\partial x_i} \frac{\partial \Omega^2}{\partial x_i} \right) \quad (\text{induced}) \quad (21)$$

where

$$\alpha = \hbar^2 [(A^2 + 2\Omega^2)G^2 - 8\Delta_e^2 \Omega^2 (4\Delta_e^2 + 5A^2 + 4\Omega^2)] / 2AG^3$$

$$\Delta_e = \Delta + \frac{\vec{p} \cdot \nabla \Theta}{m}$$

$$\beta = \hbar^2 A [G^2 - 2\Omega^2 (3A^2 - 4\Delta_e^2)] / 2G^3$$

$$\gamma = -2\hbar \Delta_e \Omega^2 (2A^2 + \Omega^2) / G^3$$

$$G = 4\Delta_e^2 + A^2 + 2\Omega^2$$

As shown, both the diffusion coefficients are tensors. The matrix  $d_{ii}^{(s)}$  is a diagonal matrix when the dipole moment is directed perpendicular to the direction of propagation of the external field. For this case and a one dimensional analysis  $j_{ii}^{(s)} = 1$  (Ref 13 pg 1087). If the form of the external field is  $E(t) = E_0 \cos(kx - \omega t)$  then equations 20 and 21 become equations 22 and 23.

$$D_s = \frac{A(\hbar k \Omega)^2}{5G} \quad (22)$$

$$D_i = \frac{\hbar^2 \Omega^2 k^2 [2\Omega^2 A(12\Delta^2 - A^2 + 2\Omega^2) + A(4\Delta^2 + A^2)^2]}{2G^3} \quad (23)$$

The physical explanation for the spontaneous diffusion coefficient is fairly straightforward. The atom spontaneously emits a photon after being excited in a time period  $\tau = \frac{1}{A}$ . This emitted photon imparts momentum to the atom. Since the direction the photon is emitted in is random, many such emissions will give rise to a walk phenomenon. Thus, a random walk in momentum space occurs. Following Rief (Ref 18 pg 488), one can calculate a diffusion coefficient which is within an order of magnitude of that obtained from equation 22. The step size is  $\hbar k$ , and the rate is  $A$ . Hence,

$$D_s = \frac{1}{2} \overline{p^2} A = \frac{(\hbar k)^2 A}{2}$$

This is within a factor of 5 of that derived from equation 20. Equation 20 evaluated in a strong field case yields,

$$D_s = \frac{1}{10} (\hbar k)^2 A$$

Since the emitted radiation pattern is dipole in nature (Ref 13 pg 1089), the diffusion coefficient due to spontaneous emission has a definite tensorial nature. That is, it has different values for different directions in space.

The induced diffusion coefficient can not be so

conveniently explained. Absorption and stimulated emission processes are not statistically independent. To absorb a photon the atom must be in a ground state. To emit a photon the atom must be in an excited state. So the probability of whether a photon emits or absorbs is dependent on what has happened in the history of the atom. Thus, the statistics of photon absorption and emission are not Poissonian (Ref 13 pg 1090).

The idea that the induced diffusion coefficient can be derived from a random walk argument is incorrect in the general case. A step size of  $\hbar k$  and a rate  $\mathcal{A}$  leads to an answer that disagrees with that found from equation 21 by a factor of  $\frac{\Omega}{A}$ . This factor can in principle be as large as desired since it is linear with the field strength. In general the induced diffusion coefficient has not yet been physically explained.

It has been pointed out that a physical explanation can be provided for certain very restricted cases (Ref 13 pg 1089). For the case of a standing wave external field that is exactly on resonance  $\Delta=0$ , a physical explanation of the induced diffusion coefficient is developed from the optical Stern-Gerlach effect.

When the external field is a standing wave and the laser is on resonance with the atomic beam, then there exists two separate distributions for the atomic beam. These two distributions are a superposition of pure quantum states for the atoms. These two distributions experience a force  $F_+$  and  $F_-$ . The states are labeled  $\psi_+$  and  $\psi_-$  for the forces they experience. The nature of the force is most easily explained by traditional

electromagnetic theory. When an electric dipole is in an external field it experiences a force  $\vec{F} = -\frac{1}{2} \nabla(\vec{\mu} \cdot \vec{E})$ . This is the magnitude of the force the atom experiences. The two distributions experience forces in the opposite direction. From the view of stimulated emission and absorption, the force arises from many coherent emissions. The probability that the atom is in either distribution is  $\frac{1}{2}$  (Ref 13 pg 1084). The force continues to interact with the beam for a time  $\tau = \frac{4}{A}$ . Since the probability the atom is in its upper state is  $\frac{1}{2}$  for the strong field case, the rate at which the atom emits is  $A/4$ . This is because the rate an atom emits is  $R = AP$ , where  $P$  is the probability the atom can emit ( $\frac{1}{2} \cdot \frac{1}{2} = \frac{1}{4}$ ).

Thus, when spontaneous emission returns the atom to its original level, the entire process can start over. The atom can once again feel a force  $\pm F$ . One can see that the beam will be split in half each time  $\sim \frac{4}{A}$ . This represents a diffusion in momentum space that can be represented as a random walk process.

For a step size in momentum space  $= \hbar \Delta \cdot \frac{4F}{A}$  and a rate of  $\frac{A}{4}$ , one obtains equation 24.

$$2D_c = \overline{(\Delta p)^2} \tau = \frac{4F^2}{A} \quad (24)$$

Thus, the diffusion coefficient as calculated from the random walk approach is

$$D_c = \frac{(\hbar \Delta)^2}{2A} \quad \text{using } |\vec{F}| = \frac{1}{2} \hbar \Delta \omega \quad (25)$$

Equation 21 gives the induced diffusion coefficient in general. For a general standing wave of the form equation 26, the induced coefficient is equation 27. For the case of exact resonance  $\Delta = 0$ , one then obtains a coefficient that is derived from the same conditions as before. This coefficient is equation 28.

$$E(\vec{r}, t) = E(x) \cos(\omega t) \quad \theta = 0 \quad (26)$$

$$D_i = \left\{ \frac{\hbar^2}{2A(4\Delta^2 + A^2 + 2\Omega^2)} \right\} \left( \frac{\partial \Omega}{\partial x} \right)^2 \cdot \left[ A^2 + 2\Omega^2 - \frac{8(4\Delta^2 + 5A^2 + 4\Omega^2)\Delta^2 \Omega^2}{(4\Delta^2 + A^2 + 2\Omega^2)^2} \right] \quad (27)$$

$$D_i = \frac{\hbar^2 (\nabla \Omega)^2}{2A} \quad \text{for } \Delta = 0 \quad (28)$$

This coefficient agrees exactly with that of equation 25 which was developed from the random walk process due to the optical Stern-Gerlach effect. It should be remembered that for off resonance cases, physical explanations do not yet yield a correct induced diffusion coefficient. Equation 21 is the general form of the induced diffusion coefficient.

In conclusion, the spontaneous diffusion coefficient (equation 20), can be explained as a random walk process in momentum space size  $\hbar k$  and rate  $A$ . The induced diffusion coefficient (equation 21), does not have a physical explanation that holds for all cases. For on resonance the Stern-Gerlach effect can be used to develop a diffusion coefficient from the random walk point of view. The total diffusion



coefficient appearing in the Fokker-Planck equation (equation 11), is the sum of the spontaneous and induced coefficients.

$$D_{total} = D_s + D_i \quad (29)$$

### Discussion

As noted above, the Fokker-Planck equation is a specialized case for a general set of coupled partial differential equations. These equations are presented below in equations 30 thru 33 for completeness.

$$\left(\frac{\partial}{\partial t} + \frac{\vec{p}}{m} \cdot \vec{\nabla}\right) S = -\frac{1}{2} \hbar (\nabla \Omega \cdot \nabla_p U + \Omega \nabla \Theta \cdot \nabla_p V) + \sum_{i,j} Q^{ij} \frac{\partial^2 (S+W)}{\partial p^i \partial p^j} \quad (30)$$

$$\left(\frac{\partial}{\partial t} + \frac{\vec{p}}{m} \cdot \vec{\nabla}\right) U = \left(\Delta + \frac{\vec{p} \cdot \vec{\nabla} \Theta}{m}\right) U - \frac{1}{2} A U - \frac{1}{2} \hbar \nabla \Omega \cdot \vec{\nabla}_p S \quad (31)$$

$$\left(\frac{\partial}{\partial t} + \frac{\vec{p}}{m} \cdot \vec{\nabla}\right) V = -\left(\Delta + \frac{\vec{p} \cdot \vec{\nabla} \Theta}{m}\right) V - \frac{1}{2} A V + \Omega W - \frac{1}{2} \hbar \Omega \nabla \Theta \cdot \vec{\nabla}_p S \quad (32)$$

$$\left(\frac{\partial}{\partial t} + \frac{\vec{p}}{m} \cdot \vec{\nabla}\right) W = -\Omega V - A(S+W) - \sum_{i,j} Q^{ij} \frac{\partial^2 (S+W)}{\partial p^i \partial p^j} \quad (33)$$

where  $Q^{ij} = \frac{1}{2} \hbar \int d^3 k \, \epsilon(k) k^i k^j \quad \vec{\nabla} = \frac{\partial}{\partial x_i} \quad \vec{\nabla}_p = \frac{\partial}{\partial p_i}$

and  $\epsilon(k) = (4\pi\hbar)^{-1} \omega \delta(\omega - \omega_0) |\mu|^2 (1 - \cos \Theta)$

in the dipole approximation.

Here  $\Theta$  is the angle between  $\vec{k}$  and  $\vec{\mu}$   $\Delta = \omega - \omega_0$  ,

$m$  is the mass of the particle and

$|\mu|$  is the dipole moment.

Equations 30 thru 33 represent the generalized quasiclassical

limit for the equation of motion for an atom in resonate conditions.

It is obvious that the Fokker-Planck equation presented in the preceeding section is easier to solve than equation 30 thru 33. The decision of which equation is to be used is based upon the exact problem under investigation. For example, a plane monochromatic running wave obviously fullfills the requirements for the smooth field approximation. Thus, the Fokker-Planck equation could be used to investigate this problem as long as the time scale under consideration was long compared to  $1/\Delta$ . On the other hand, a problem with a standing wave external field in which the atom moves a significant distance compared to the distance over which the field changes amplitude, would require that equations 30 thru 33 be solved. So the optical Stern-Gerlach effect can not be predicted using the Fokker-Planck equation.

In conclusion, there exists a set of generalized equations of motion for a two level atom in an external field (Ref 13 pg 1082). These integral equations include all effects of field quantization. The quasiclassical limit (Ref 13 pg 1083) of these equations are presented here as equation 30 thru 33. The use of Ehrenfests theorem and a form for the applied field, yield the optical-Bloch equations (equations 8 thru 10). The optical Bloch equations are consistant with the generalized set of equations but only predict the equation of motion of the centroid of the atomic wave packet (Ref 11 pg 227). That is, they will not predict such results as the optical Stern-

Gerlach effect which is quantum mechanical in nature. For the smooth field approximation (Ref 13 pg 1096), equations 30 thru 33 reduce to the Fokker-Planck equation (equation 11) with force and diffusion coefficients given by equations 15 and 29 respectively. The Fokker-Planck equation is accurate to second order in  $\hbar$ . For the case of a plane monochromatic traveling wave interacting with an atomic beam, the Fokker-Planck equation is sufficient to solve the equation of motion of the atomic beam distribution function. The analysis section takes this example and presents the numerical solution of the Fokker-Planck equation for this case.

### III. Application of the Theory to Cooling an Atomic Beam

#### Introduction

This section deals with the application of the theory developed in section II, to the problem of using a laser in resonance with the atomic beam to decrease its speed. Following this introduction, the Fokker-Planck equation will be converted from a partial differential equation into a difference equation. The numerical solution of this difference equation is studied in view of the constraints imposed upon the step sizes of time and velocity, due to convergence and stability of the numerical solution. A description of the particular case studied and its initial conditions are then given. The difference equation is solved numerically and compared to experimental results.

#### The Fokker-Planck Equation as a Difference Equation

As shown in section II, the Fokker-Planck equation serves as a method of calculating the time history of the atomic beam distribution function in cases where the smooth field approximation applies. One method of numerically solving this equation is to convert it to a difference equation and solve using the method of finite differences.

If the differentials in the Fokker-Planck equation are replaced by difference quotients, the resulting equation is known as a difference equation. Deriving these difference quotients is straightforward. If there exists a function  $\psi$  that has continuous fourth derivatives, then it is expandable in a Taylor series expansion as in equations 34 and 35.

$$f(x_1+h) = f(x_n) + f'(x_n)h + \frac{f''(x_n)h^2}{2} + \frac{f'''(x_n)h^3}{6} + \frac{f^{(4)}(\xi_1)h^4}{24} \quad x_n < \xi_1 < x_n+h \quad (34)$$

$$f(x_1-h) = f(x_n) - f'(x_n)h + \frac{f''(x_n)h^2}{2} - \frac{f'''(x_n)h^3}{6} + \frac{f^{(4)}(\xi_2)h^4}{24} \quad x_n-h < \xi_2 < x_n \quad (35)$$

Here  $h$  is the step size. To find difference quotients for  $f'(x_n)$  or  $f''(x_n)$ , one solves equations 34 and 35 for the derivative wanted. For instance, if equation 35 is added to 34 and subtracted from the resulting sum, one obtains equation 36.

$$f(x_n+h) + f(x_n-h) - 2f(x_n) = f''(x_n)h^2 + \frac{h^4}{24} [f^{(4)}(\xi_1) + f^{(4)}(\xi_2)] \quad (36)$$

Here  $f(x_n+h)$  means the function evaluated at the value  $x_n+h$ , where  $h$  is an arbitrary step size. This is rewritten in equation 37 as,

$$f''(x_n) = \frac{f(x_n+h) - 2f(x_n) + f(x_n-h)}{h^2} + O(h^2) \quad (37)$$

$O(h^2)$  means that the error approaches proportionally to  $h^2$  as  $h \rightarrow 0$ . This is known as a central difference formula for the second derivative (Ref 14 pg 219), since the derivative at point  $x_n$  depends on values of the function at velocity points before and after it. A forward difference formula for the first derivative is derived from equation 34 by solving directly for  $f'(x_n)$  as in equation 38.

$$f'(x_n) = \frac{f(x_n+h) - f(x_n)}{h} + O(h) \quad (38)$$

As shown, this has errors proportional to  $h$ . Finally, a central difference formula for the first derivative is given in 39.

$$f'(x_n) = \frac{f(x_n+h) - f(x_n-h)}{2h} + O(h^2) \quad (39)$$

Corresponding to equations 37 thru 39, are similar equations with the variable  $t$  replacing  $x$ . Obviously, the choice of variable is immaterial.

To allow use in a partial differential equation, the difference equations must be modified. To solve the Fokker-Planck equation in one dimension, assume arbitrary step sizes for time and position. Thus,  $f(x_n, h)$  becomes  $f(x_n + \Delta x_n)$ , and  $f(t, h)$  becomes  $f(t + \Delta t)$ . Partial derivatives with respect to time and space can then be written as equation 40 thru 42.

$$\frac{\partial f}{\partial t} = \frac{f(t + \Delta t) - f(t)}{\Delta t}, \text{ forward difference.} \quad (40)$$

$$\frac{\partial f}{\partial v} = \frac{f(v + \Delta v) - f(v - \Delta v)}{2 \Delta v}, \text{ central difference.} \quad (41)$$

$$\frac{\partial^2 f}{\partial v^2} = \frac{f(v + \Delta v) - 2f(v) + f(v - \Delta v)}{\Delta v^2}, \text{ central difference.} \quad (42)$$

Again the choice of variable is of no substantial consequence. The only assumption is that the function has continuous fourth derivatives for the variable in question.

Many difference equations can be written for one partial differential equation by using different combinations of forward, central, and even backwards difference equations for the partials. The Fokker-Planck equation must be solved for successive increments in time and velocity. Thus, a forward or central difference must be used. To ease calculations and file space, a forward difference will be used for the partial with respect to time. The second derivative must be written as a central difference if one wishes to avoid using a first derivative to calculate the second derivative. The choice of forward or central difference for the first partial with respect to velocity is at this time arbitrary and will be left for later.

A time and velocity plane is constructed to solve the Fokker-Planck equation. The axes are scaled from 0 to as large as desired in increments of  $\Delta t$  and  $\Delta v$ . The partial derivatives presented in equations 40 thru 42 are written again in equations 43 to 45.

$$\frac{\partial S_i^j}{\partial t} = \frac{S_{i+1}^j - S_i^j}{\Delta t} \quad , \text{forward difference. (43)}$$

$$\frac{\partial S_i^j}{\partial v} = \frac{S_{i+1}^j - S_{i-1}^j}{2 \Delta v} \quad , \text{central difference. (44)}$$

$$\frac{\partial^2 S_i^j}{\partial v^2} = \frac{S_{i+1}^j - 2S_i^j + S_{i-1}^j}{\Delta v^2} \quad , \text{central difference. (45)}$$

The superscripts denote the time position at which the function

is to be evaluated. The subscripts refer to the velocity position at which the function is to be evaluated. All the equations necessary to write the Fokker-Planck as a difference equation are now present. Two difference equations for the Fokker-Planck equation are presented in equations 46 and 47. In both equations, the time partial is a forward difference and the second partial with respect to velocity, is a central difference. The only difference between the two is how the first partial with respect to velocity is represented. In both equations the force and diffusion coefficients have sub and super scripts since in general they depend on time and velocity.

$$\frac{f_i^{j+1} - f_i^j}{\Delta t} = - \left[ \frac{F_{i+1}^j f_{i+1}^j - F_i^j f_i^j}{m \Delta v} \right] + \left[ \frac{D_{i+1}^j f_{i+1}^j - 2D_i^j f_i^j + D_{i-1}^j f_{i-1}^j}{m^2 \Delta v^2} \right] \quad (46)$$

$$\frac{f_i^{j+1} - f_i^j}{\Delta t} = - \left[ \frac{F_{i+1}^j f_{i+1}^j - F_{i-1}^j f_{i-1}^j}{2m \Delta v} \right] + \left[ \frac{D_{i+1}^j f_{i+1}^j - 2D_i^j f_i^j + D_{i-1}^j f_{i-1}^j}{m^2 \Delta v^2} \right] \quad (47)$$

The Fokker-Planck equation is a parabolic differential equation (Ref 19). Thus, the equation is solvable using the explicit method of finite differences (Ref 14 pg 220). This means that when the partials are replaced by the difference quotients, the value of the function at the  $i$ th velocity can be solved explicitly for the  $j + 1$ th time. This is evident from 46 and 47. All values in the equation are known except for  $f_i^{j+1}$ .

The initial atomic distribution function is given by Ramsey (Ref 12). This represents the atomic velocity distribution function as it comes out of the atomic oven. This



distribution function will be changed as time proceeds as prescribed by equations 46 and 47. The general forms for  $F_1^0$  and  $D_1^0$  are given by equations 15 and 29. The explicit values used for the force and diffusion coefficient depend upon the exact problem to be solved. The next subsection discusses the particular case to be examined and derives explicit equations for  $F_1^1$  and  $D_1^1$ .

#### Slowing an Atomic Beam Using A Scanning Frequency Laser

Consider a monochromatic plane traveling wave counter-propagated against a collimated atomic beam. The form of the wave is given in 48.

$$E(\bar{x}) = E_0 \cos(\bar{k} \cdot \bar{x} - \omega t) \quad (48)$$

The force of interaction between the field and the beam is given in 49.

$$\bar{F} = \frac{A \Omega^2 \hbar k}{[4(\Delta + kv)^2 + A^2 + 2\Omega^2]} = - \frac{A \Omega^2 \hbar k \hat{k}}{[(\Delta + kv)^2 + A^2 + 2\Omega^2]} \quad (49)$$

The total diffusion coefficient was derived in equations 22 and 23. It is given here as equation 50.

$$D_L = \frac{\hbar^2 A \Omega^2 k^2}{5[4(\Delta + kv)^2 + A^2 + 2\Omega^2]} + \frac{\hbar^2 \Omega^2 k^2}{2[4(\Delta + kv)^2 + A^2 + 2\Omega^2]^3} \left\{ 2\Omega^2 A \right. \\ \left. \cdot [12(\Delta + kv)^2 - A^2 + 2\Omega^2] + [4(\Delta + kv)^2 + A^2]^2 \right\} \quad (50)$$

This problem is treated in one dimension since the wave is assumed to be of infinite extent and constant strength  $\Omega$ .

The wave vector  $\vec{k} = -|\vec{k}|\hat{k}$ , since the laser is counter-propagated against the beam.

In both equations there is a term  $\Delta + kv$ . This is the effective detuning since  $\Delta = \omega - \omega_0$  and  $-kv$  is the doppler shift term. The laser starts at a frequency tuned to resonance with the initial velocity atoms  $v_0$ . The effective detuning is zero at the peak of the force. As the laser frequency is swept, different velocities come into resonance with the laser. That is, different velocities make the effective detuning equal to zero. The force is maximized when the effective detuning is zero.

$$\Delta + kv_p = 0, \quad v_p \text{ represents the velocity at peak force. (51)}$$

At time  $t=0$ , the velocity  $v=v_0$ , so that

$$\Delta = -kv_0 \quad (52)$$

The force then assumes the form

$$\vec{F} = -\frac{A\Omega^2 \hbar \vec{k} \hat{k}}{A^2 + 2\Omega^2} \quad (53)$$

If the laser frequency changes, then  $\Delta$  changes in a manner yet to be determined. As  $\Delta$  changes, different velocities will satisfy equation 51. Thus, the force will be resonant (i.e. a maximum), for different velocities of the atomic velocity

distribution function as the frequency of the laser is changed. The force is opposite the beam so the atoms are slowed. If the laser frequency is changed so that the atoms in the beam slow just enough to remain at the peak of the force, then

$$\bar{F} = m \bar{v} = - \frac{A \Omega^2 \hbar k \hat{k}}{A^2 + 2 \Omega^2} \quad (54)$$

Integrating 54 yields a velocity at which the force is maximized at

$$v_p = v_0 - \frac{A \Omega^2 \hbar k t}{m(A^2 + 2 \Omega^2)} \quad (55)$$

Here  $v_0$  is a constant of integration and equals the initial velocity that is on resonance. Equation 51 gives another relation for the velocity at the peak of the force. Combining these two yields

$$\Delta = -k v_p = -k \left[ v_0 - \frac{A \Omega^2 \hbar k t}{m(A^2 + 2 \Omega^2)} \right] \quad (56)$$

So if the atoms stay in resonance with the force, then the detuning changes with the scanning frequency of the laser as

$$\Delta = -k v_0 + R t, \text{ where } R = \frac{A \Omega^2 \hbar k^2}{m(A^2 + 2 \Omega^2)} \quad (57)$$

This is the detuning rate at which the atoms slow just enough to stay in resonance with the laser. If the rate is any faster

the atoms will not be slowed enough to stay with the peak force. The detuning rate should be less than the maximum calculated in 57. This indicates the inequality

$$R < \frac{A\Omega^2 \hbar k^2}{m(A^2 + 2\Omega^2)}, \quad R \text{ has units of } \text{sec}^{-2} \text{ in MKS.} \quad (58)$$

The physics of the problem are now established. A laser interacting with an atomic beam which is characterized by its distribution function  $\xi$ , exerts a force given by 49. The laser initially is in resonance with an initial velocity  $v_0$ . The laser frequency is swept at a rate given by 58. This causes atoms to slow down and the velocity distribution function is changed. A diffusion coefficient given by equation 50, causes heating and moves atoms out of the peak of the force. As the laser frequency decreases, substantial numbers of atoms are slowed to lower velocities. The final velocity the atoms are slowed to is proportional to the doppler shift  $\Delta v = \frac{\Delta \omega}{k}$ . The force in equation 49 is Lorentzian in  $\omega$ . Thus, it has a characteristic full width at half maximum spread in frequency of  $(A^2 + 2\Omega^2)^{1/2}$ . This corresponds to natural and power broadening of the force due to the atomic response (Ref 11 pg 226). For typical numbers, this is much narrower than the FWHM of the initial distribution function. So as the laser is swept in frequency, the distribution function becomes narrower and moves to a slower velocity.

### Stability and Convergence Analysis

As mentioned before, the step sizes for  $\Delta t$  and  $\Delta v$  are arbitrary within limits set by stability and convergence criteria. The convergence criteria are derived using the principal that the numerical solution approaches the real solution as  $\Delta v$  and  $\Delta t$  tend toward 0. Stability is defined as the damping of error terms as they propagate through the calculations in time. The two difference equations introduced in equations 46 and 47 are investigated for convergence criteria first, then for stability. The two equations are then compared and the one that has the least stringent requirements on  $\Delta t, \Delta v$  is chosen to solve the Fokker-Planck equation.

The equations needed for the convergence and stability analysis are equations 59 thru 61. Equation 59 is the Fokker-Planck equation. Equation 60 is the Fokker-Planck equation rewritten as a difference equation, with a forward difference used on the first partials, and a central difference used on the second partial with respect to velocity, henceforth called method 1. Equation 61 is a difference equation, with the velocity partials written as central differences, and the partial with respect to time, written as a forward difference, henceforth called method 2.

$$\frac{\partial f}{\partial t} = -\frac{\partial}{\partial v} (F f) + \frac{\partial^2}{\partial v^2} (D f) \quad (59)$$

$$f_i^{j+1} - f_i^j = -\frac{\Delta t}{m \Delta v} [F_{i+1}^j f_{i+1}^j - F_i^j f_i^j] + \frac{\Delta t}{\Delta v^2} \left[ \frac{D_{i+1}^j f_{i+1}^j - 2 D_i^j f_i^j + D_{i-1}^j f_{i-1}^j}{m^2} \right] \quad (60)$$

$$s_n^{j+1} - s_n^j = -\frac{\Delta t}{m \Delta v} \left[ \frac{F_{n+1}^j s_{n+1}^j - F_n^j s_n^j}{2} \right] + \frac{\Delta t}{\Delta v^2} \left[ \frac{D_{n+1}^j s_{n+1}^j - 2D_n^j s_n^j + D_{n-1}^j s_{n-1}^j}{m^2} \right] \quad (61)$$

As before, the superscripts refer to time increments and the subscripts refer to velocity increments. From now on, the convention will be used that all superscripts will be dropped unless they do not equal  $j$ . Therefore, all difference equations will have only one term with superscripts. The convergence analysis for methods 1 and 2 follow.

The exact solution to the differential equation is  $u_n^j$  and the numerical solution is  $s_n^j$ . The error involved with substituting the numerical for the real solution is  $e_n^j$ .

Thus,

$$e_n^j = u_n^j - s_n^j$$

$$, \text{ and } s_n^j = u_n^j - e_n^j .$$

To analyze the convergence constraint for method 1, substitute the above relation into 60 and collect terms to obtain

$$\begin{aligned} e_n^{j+1} = & u_n^{j+1} + \left[ r \left( \frac{D_{n+1}^j e_{n+1}^j + D_n^j e_n^j}{m^2} \right) - \frac{r \Delta v}{m} F_{n+1}^j e_{n+1}^j \right] + e_n^j \left[ 1 - \frac{2r D_n^j}{m^2} + \frac{F_n^j r \Delta v}{m} \right] \\ & + \left[ -r \left( \frac{D_{n+1}^j u_{n+1}^j + D_n^j u_n^j}{m^2} \right) + \frac{r \Delta v}{m} F_{n+1}^j D_{n+1}^j \right] \\ & - u_n^j \left[ 1 + \frac{2r D_n^j}{m^2} + \frac{r \Delta v}{m} F_n^j \right] \end{aligned} \quad (62)$$

Here  $r = \frac{\Delta t}{\Delta v^2}$ . A Taylor series expansion of  $u_{n+1}^j, u_n^j, u_{n-1}^j$  yields

$$v_{n+1}^j = v_n^j + \left(\frac{\partial v}{\partial v}\right) \Delta v + \frac{\Delta v^2}{2} \frac{\partial^2 v}{\partial v^2}(\xi_1, t) \quad v_n < \xi_1 < v_{n+1}$$

$$v_{n+1}^j = v_n^j - \left(\frac{\partial v}{\partial v}\right) \Delta v + \frac{\Delta v^2}{2} \frac{\partial^2 v}{\partial v^2}(\xi_2, t) \quad v_{n+1} < \xi_2 < v_n$$

$$v_n^{j+1} = v_n^j + \frac{\partial v}{\partial t}(v_n, \tau) \quad t^j < \tau < t^{j+1}$$

Substitute the above relations into 62 and cancel the appropriate terms to obtain 63.

$$e_n^{j+1} = \left[ r \left( \frac{D_{n+1}^j e_{n+1}^j + D_n^j e_n^j}{m^2} \right) - \frac{r \Delta v}{m} F_{n+1}^j e_{n+1}^j \right] + e_n^j \left[ 1 - \frac{2r D_n^j}{m^2} + \frac{r \Delta v}{m} F_n^j \right] + \Delta t M \quad (63)$$

$$\begin{aligned} \text{Here } M = & \frac{\partial v}{\partial t}(v_n, \tau) + \left[ -\frac{1}{\Delta v^2} \left( \frac{D_{n+1}^j}{m^2} \xi v_n^j + \frac{\partial v}{\partial v} \Delta v + \frac{\partial^2 v}{\partial v^2}(\xi_1, t) \frac{\Delta v^2}{2} \right) \right. \\ & + \frac{D_n^j}{m^2} \xi v_n^j + \frac{\partial^2 v}{\partial v^2}(\xi_2, t) \frac{\Delta v^2}{2} - \frac{\partial v}{\partial v}(\Delta v) \left. \right] + \frac{1}{\Delta v m} F_{n+1}^j \cdot \left[ v_n^j - \frac{\partial v}{\partial v} \Delta v \right. \\ & \left. + \frac{\partial^2 v}{\partial v^2}(\xi_1, t) \frac{\Delta v^2}{2} \right] - v_n^j \left( \frac{2 D_n^j}{m^2} + \frac{F_n^j}{m \Delta v} \right) \end{aligned}$$

with all  $r$ 's expressed as  $r = \frac{\Delta t}{\Delta v^2}$ .

The magnitude of the maximum error in time  $t^j \rightarrow t^{j+1}$  is  $E^{j+1} - E^j$ . To calculate this error, take the maximum values in equation 63 and the magnitude of  $M$ .

$$E^{j+1} = \left[ \left( \frac{r D_m^j}{m^2} E^j + \frac{r D_m^j}{m^2} E^j \right) - \frac{r \Delta v}{m} F_m^j E^j \right] + E^j \left[ 1 - \frac{2r D_m^j}{m^2} + \frac{r \Delta v}{m} F_m^j \right] + \Delta t |M| \quad (64)$$

where  $D_m^j$  and  $F_m^j$  are the maximum values of  $D_n^j$  and  $F_n^j$ .

This leads directly to 65.

$$E^{j+1} = E^j \left[ \frac{2r D_m^j}{m^2} - \frac{r \Delta v}{m} F_m^j \right] + E^j \left[ 1 - \frac{2r D_m^j}{m^2} + \frac{r \Delta v}{m} F_m^j \right] + \Delta t |M| \quad (65)$$

If the coefficients of  $E^j$  and  $|M|$  are positive, then the following inequality holds.

$$E^{j+1} \leq \left[ \frac{2cD_m}{m^2} - \frac{r\delta v f_m}{m} + \frac{r\delta v f_m}{m} - \frac{2cD_m}{m^2} \right] E^j + E^j + \delta t |M| \quad (66)$$

and thus,  $E^{j+1} \leq E^j + \delta t |M|$ . Applying this result at different times leads to 67.

$$E^{j+1} \leq E^j + \delta t |M| \leq E^{j-1} + 2\delta t |M| \leq \dots \leq E^0 + (j+1)\delta t |M| \quad (67)$$

The last term  $E^0 + (j+1)\delta t |M| = (j+1)\delta t |M|$  since  $E^0 = 0$  at time  $t^j = 0$ .

Equation 67 shows the difference equation will converge to the real solution after  $j$  iterations. This will happen when initial errors are zero and when  $\delta t$  is arbitrarily small with  $|M|$  finite. The initial condition in this problem is the velocity distribution function, which is theoretically and experimentally well known. So the initial errors can be made zero. The term can go to 0 as  $\delta t$  goes to 0 as long as  $|M|$  is finite.  $|M|$  is given in 63 and by inspection it is finite as long as  $\delta v$  and  $m \neq 0$ .

As pointed out above, the coefficients of  $E^j$  and  $|M|$  must be positive for 66 and 67 to hold true. So the convergence criteria are found from requiring that the coefficients be positive. Therefore,



$$\left[ \frac{2r D_m}{m^2} - \frac{r \Delta v F_m}{m} \right] > 0$$

$$\left[ 1 - \frac{2r D_m}{m^2} + \frac{r \Delta v F_m}{m} \right] > 0$$

$$\Delta t > 0$$

$$\text{Now } D_{\max} = D_m = \frac{k^2}{2(A^2 + 2\Omega^2)} \left[ \Omega^2 k^2 (2\Omega^2 A^2 - A^2 + 2\Omega^2 \zeta + A^2) \right] + \frac{A(k\omega\Omega)^2}{5\epsilon^2(A^2 + 2\Omega^2)}$$

$$\text{and } F_{\max} = F_m = - \frac{A\Omega^2 k k}{A^2 + 2\Omega^2}$$

Obviously  $D_{\max}$  can be made positive since the Rabi frequency can be made larger than the Einstein A coefficient. Equally obvious, the term  $F_{\max}$  is always negative for this case. Thus, the first and third equations can provide no constraints upon the difference equation. The second equation is the only equation that can provide such a constraint. To find this constraint, solve the inequality for  $r$ . Replace  $r$  with its value  $r = \frac{\Delta t}{\Delta v}$ . Upon doing this one obtains

$$\Delta t < \frac{(m \Delta v)^2}{[2 D_m + m \Delta v |F_m|]} \quad (68)$$

These are the convergence criteria for method 1.

The convergence criteria for method 2 are found in much the same way. Let the real solution corresponding to the differential equation be  $\mathcal{U}_n^i$ . The solution to the difference equation is  $\xi_n^i$ . The error involved is  $\epsilon_n^i$ . This leads again to  $\xi_n^i = \mathcal{U}_n^i - \epsilon_n^i$ .

Substitute this into 61 and obtain 69.

$$e_n^{j+1} = u_n^{j+1} + \left[ e_n^j \left( 1 - \frac{2r D_n^j}{m^2} \right) + e_{n+1}^j \left( -\frac{rav F_{n+1}^j}{m} + \frac{r D_{n+1}^j}{m^2} \right) + e_{n-1}^j \left( \frac{rav F_{n-1}^j}{m} + \frac{r D_{n-1}^j}{m^2} \right) \right] + \left[ u_{n+1}^j \left( -1 + \frac{2r D_n^j}{m^2} \right) + u_{n-1}^j \left( \frac{rav F_{n+1}^j}{2m} - \frac{r D_{n+1}^j}{m^2} \right) + u_n^j \left( -\frac{rav F_{n-1}^j}{m} - \frac{r D_{n-1}^j}{m^2} \right) \right] \quad (69)$$

Expand the terms  $u_{n+1}^j$ ,  $u_n^j$ ,  $u_{n-1}^j$ , as Taylor series as before. Collect all terms in  $u$  and express them as  $M$ . Equation 69 then becomes 70.

$$e_n^{j+1} = \left[ e_n^j \left( 1 - \frac{2r D_n^j}{m^2} \right) + e_{n+1}^j \left( -\frac{rav F_{n+1}^j}{2m} + \frac{r D_{n+1}^j}{m^2} \right) + e_{n-1}^j \left( \frac{rav F_{n-1}^j}{m} + \frac{r D_{n-1}^j}{m^2} \right) \right] + \Delta t M \quad (70)$$

$$\text{Where } M = \left[ \frac{\partial u}{\partial t}(v_n, \eta) + \frac{2 D_n^j u_n^j}{m^2 \Delta v^2} + \left( u_n^j + \frac{\partial u}{\partial v} \Delta v + \frac{\Delta v^2}{2} \frac{\partial^2 u}{\partial v^2}(\xi, t) \right) \cdot \left( \frac{F_{n+1}^j}{2m \Delta v} - \frac{D_{n+1}^j}{\Delta v^2 m^2} \right) + \left( u_n^j - \frac{\partial u}{\partial v} \Delta v + \frac{\Delta v^2}{2} \frac{\partial^2 u}{\partial v^2}(\xi, t) \right) \cdot \left( \frac{F_{n-1}^j}{2m \Delta v} - \frac{D_{n-1}^j}{\Delta v^2 m^2} \right) \right]$$

The maximum magnitude of the error for the calculation at time  $t^j$  is  $E^j$ , so that once again,

$$E^{j+1} \leq E^j + \Delta t |M| \leq E^{j+1} + 2 \Delta t |M| \leq \dots \leq E^0 + \Delta t |M| = \Delta t |M|$$

This is true if all coefficients of the error term are positive. This gives the constraint upon  $r$  such, that the solution from the difference solution converge to the solutions of the differential equation.

$$\left( 1 - \frac{2r D_m}{m^2} \right) > 0 \quad \text{or} \quad \Delta t < \frac{(m \Delta v)^2}{2 D_m} \quad (71)$$

Equations 68 and 71 represent the constraints upon methods 1 and 2 respectively for the solutions of the difference equations to converge to the solutions of the differential equation.

The stability constraints are now obtained. Expand the velocity distribution function as a fourier lattice series (Ref 20 pg 3). One then obtains 72.

$$f_n = \sum_k A_n \exp\{i\theta(k)n\} = \sum_k A_n v_n(k) \quad , \text{ where } v_n(k) = e^{i\theta(k)n} \quad (72)$$

and  $\theta(k) = \sin k$  .

The subscripts denoting velocity have been changed to n since a complex term has been introduced. Equation 72 shows that the distribution function at velocity n is a series of fourier components. Each component in this expansion is a solution to 60 and 61. If the coefficients are constant then each component of this series can be seen to be a eigenfuncton of equations 60 and 61. Substitute the component  $v_n(k)$  into 60 and obtain

$$v_n^{j''} = v_n^j \left[ 1 + \frac{r D_m}{m^2} (e^{i\theta} + e^{-i\theta}) - \frac{2r D_m}{m^2} + \frac{r \partial v f_m}{m} - \frac{r \partial v f_m}{m} e^{i\theta} \right] \quad (73)$$

Obviously, the term in brackets is the eigenvalue. So each component of the expansion conforms to equation 74.

$$v_n^{j''} = \lambda v_n^j \quad (74)$$

Equation 60 and 61 show that each value of the velocity distribution function for time  $t, t^{j''}$  is calculated using

existing values of the distribution function at different velocities. If an error is introduced as calculations proceed, because of round off errors or other problems, then it affects subsequent calculations. The error is

$$e_n^j = u_n^j - \overline{u_n^j}, \text{ where } \overline{u_n^j} \text{ is the value that is incor- (75)}$$

rect at time  $j$  and velocity  $n$ . This error term will give solutions to equation 60 of the same form as 74 except that  $u_n^{j+1}$  will be  $e_n^{j+1}$ . Starting with 74 and  $e_n^{j+1}$  instead of  $u_n^{j+1}$  at time  $t^0$ ,  $e^1 = \lambda e^0$ .

For the next time iteration one obtains

$$e^2 = \lambda e^1 = \lambda^2 e^0 \quad (76)$$

Here the superscripts on the  $e$ 's are time increments and the superscripts on the  $\lambda$ 's are exponents. For each time iteration, the error is multiplied by the eigenvalue  $\lambda$ .

Stability for numerical calculations means that as successive calculations are made, the errors tend to damp out. Looking at 76, one sees that after  $j$  iterations

$$e^j = \lambda^j e^0 \quad (77)$$

If due to the initial error  $e^0$ , one requires that after  $j$  iterations  $e^j < \lambda^j e^0$ , then obviously  $|\lambda| < 1$ . If  $|\lambda| > 1$  then the errors grow instead of decrease. To find the requirement

for stability then, one requires that

The constraint upon method 1 is then

$$\left| 1 + \frac{2rD_m}{m^2} (\cos \Theta - 1) + \frac{r\Delta v F_m}{m} (1 - \cos \Theta) + \frac{r\Delta v F_m}{m} i \sin \Theta \right| < 1 \quad (78)$$

This simply states that the eigenvalue found in 73 has a magnitude less than 1. Euler's relations have been used when writing 78 to turn the exponents into sin's and cos's.

Calculating the indicated magnitude is tedious but straightforward. The real and imaginary parts of the equation are squared and added together. The square root of the resulting quadratic is the magnitude. After this, one solves for  $r$  and obtains 79.

$$r < \frac{\frac{4D_m}{m^2} - \frac{2\Delta v F_m}{m}}{\left[ \left( \frac{4D_m}{m^2} - \frac{4D_m F_m \Delta v}{m^2} \right) (1 - \cos \Theta) + \frac{2F_m^2 \Delta v^2}{m^2} \right]} \quad (79)$$

This calculation is made for one particular  $\mathcal{U}_n$ . Since the value of the velocity distribution is a sum of a series of the  $\mathcal{U}_n$ 's, each  $\mathcal{U}_n$  must remain stable. The errors must not be growing in any of the components of the series, or these errors will swamp out all the other components. For every value of  $\Theta$ , equation 79 must be true or the difference equation will be unstable. Thus, every value of  $\Theta$  that gives a unique value to 79 must be satisfied. Following Kittel (Ref 20 pg 3), the allowed values of  $\Theta$  are given by the periodic boundary condition that

$$u_{n+N} = u_n \quad (80)$$

$$\begin{aligned} \text{So } \exp \{ i \Theta (n+N) \} &= \exp \{ i \Theta n \} \\ \Rightarrow \exp \{ i \Theta N \} \exp \{ i \Theta n \} &= \exp \{ i \Theta n \} \end{aligned}$$

This will only be true if  $\exp \{ i \Theta N \} = 1$  or  $\Theta N = \pm \pi$ .

So the values of  $\Theta$  that are allowed are

$$-\pi < \Theta < +\pi \quad \text{or} \quad -\pi < \Delta v k < +\pi \quad (81)$$

Since 79 must be satisfied for all values of  $\Theta$ , only the most stringent requirement on the inequality is important. Since  $\propto \frac{\Delta t}{\Delta v}$  in 79, it can be seen that what this equation really means is that  $\Delta t$  must be smaller than a definite number for every value of  $\Delta v$ . The most stringent requirement corresponds to the smallest  $\Delta t$  that is calculable. To minimize the  $\Delta t$ , the  $(1 - \cos \Theta)$  term must be maximized. The maximum value for this term is 2. Place this in 79 to obtain the constraint on  $\Delta t$  for method 1.

$$\Delta t < \frac{\Delta v^2 \left[ \frac{4D_m}{m^2} - \frac{2\Delta v F_m}{m} \right]}{\left[ 2 \left( \frac{4D_m^2}{m^4} - \frac{4F_m D_m \Delta v}{m^3} \right) + \frac{2F_m^2 \Delta v^2}{m^2} \right]} \quad (82)$$

which becomes  $\Delta t < \frac{(m\Delta v)^2}{(2D_m + \Delta v m |F_m|)}$  upon cancellation of appropriate terms. The terms cancel since  $F_{\max} = - |F_{\max}|$ .

Inspection of 68 and 82 show the criteria for convergence and stability are the same for method 1.

The stability criteria for method 2 are found in a similar manner. Insert equation 72 into 61 to obtain

$$S_n^{(1)} = e^{i\theta n} \left[ 1 - \frac{2rD_m}{m^2} + \frac{r\Delta v F_m}{2m} (-e^{i\theta n} + e^{-i\theta n}) + \frac{rD_m}{m^2} (e^{i\theta} + e^{-i\theta}) \right] \quad (83)$$

Using Euler's relation

$$S_n^{(1)} = e^{i\theta n} \left[ 1 - \frac{2rD_m}{m^2} + \frac{2rD_m \cos \theta}{m^2} - \frac{ir\Delta v F_m \sin \theta}{m} \right], \text{ where } \theta = \Delta v k \quad (84)$$

The term in brackets is the eigenvalue. As before its magnitude must be less than 1 for stability. So the constraint upon method 2 is

$$\left[ 1 + \frac{4rD_m}{m^2} (\cos \theta - 1) + \frac{4r^2 D_m^2}{m^4} (1 - \cos \theta) + \frac{r^2 \Delta v^2 F_m^2 \sin^2 \theta}{m^2} \right]^{1/2} < 1 \quad (85)$$

Solving this inequality for  $r$  and remembering that  $r = \frac{\Delta t}{\Delta v}$ , one obtains 86. This is the constraint upon the time increment vs the velocity increment for method 2 due to stability requirements.

$$\Delta t \leq \frac{4 D_m \Delta v^2}{\left[ \left( \frac{4 D_m^2}{m^4} + \frac{F_m^2 \Delta v^2}{m^2} \right) + \left( \frac{F_m^2 \Delta v^2}{m^2} - \frac{4 D_m^2}{m^4} \right) \cos \theta \right]} \quad (86)$$

Once again, all terms of the expansion must obey the requirement that they not have errors growing as calculations proceed.

Thus, all values of  $\cos \Theta$  must be examined and the most stringent satisfied in 86. The maximum value for  $\cos \Theta$  is  $\pm 1$ , and now

$$\Delta t \leq \frac{2 D_m}{|F_m|} \quad \text{for } \cos \Theta = 1, \text{ or } (87)$$

$$\Delta t \leq \frac{(m a v)^2}{2 D_m} \quad \text{for } \cos \Theta = -1.$$

These criteria agree with Roach (Ref 21 pg 45).

The above stability analysis is valid only for local conditions. An eigenvalue must be constant for a given problem. Both the eigenvalues 73 and 84 contain the terms  $F_{\max}$  and  $D_{\max}$ . In the original equation these terms depend on velocity and time. The constant values of the peak force and diffusion coefficient were used so that the calculations could be performed. Thus, the stability analysis is really only valid for regions where the force and diffusion coefficients remain constant with respect to their current values. This requirement is met if the step sizes for velocity and time are small enough to limit the change in force and diffusion. So overall constraints on the step sizes are given by the requirement that the force and diffusion coefficient can not change drastically over the step size. This leads to the term local stability. If the local stability conditions are not met, then certainly overall stability can not be insured. Thus, local stability is a necessary, but not sufficient condition



for overall stability.

The two methods are now compared to determine which has the least stringent requirement on the time vs velocity step size. An initial step size will be used, that insures the force and diffusion coefficients do not change significantly over the step size. The most stringent constraint on each method will be compared to see which offers the largest time vs velocity step size. Comparing the most stringent constraints will insure that all stability and convergence criteria are met. Picking the method that has the least stringent of these constraints promises faster run times.

Equation 88 shows the requirement for stability and convergence for method 1. Equations 89 and 90 give the requirement for convergence and stability respectively for method 2.

$$\Delta t < \frac{(m \Delta v)^2}{(2 D_m + m \Delta v |F_m|)} \quad (88)$$

$$\Delta t < \frac{(m \Delta v)^2}{2 D_m} \quad (89)$$

$$\Delta t < \frac{2 D_m}{|F_m|^2}, \text{ or } \Delta t < \frac{(m \Delta v)^2}{2 D_m} \quad (90)$$

From before we know that  $D_m$  is

$$D_m = \frac{h^2}{2(A^2 + 2\Omega^2)} \left[ \Omega^2 k^2 (2\Omega^2 A^2 - A^2 + 2\Omega^2) + A^4 \right] + \frac{A(h\omega\Omega)^2}{5c^2(A^2 + 2\Omega^2)} \quad (91)$$

and  $F_m$  is

$$F_m = - \frac{A(\Omega^2 h k)}{(A^2 + 2\Omega^2)} \quad (92)$$

For any realistic case,  $\Omega$  is 5-10 times larger than  $A$ . After discarding insignificant terms, an order of magnitude calculation for on resonance will yield

$$D_m = \frac{h^2 \Omega^2 k^2 (4\Omega^4 A)}{2(2\Omega^2)^3} = \frac{(hk)^2 A}{4} \quad \text{and} \quad (93)$$

$$F_m = - \frac{A\Omega^2 h k}{2\Omega^2} = - \frac{A h k}{2} \quad (94)$$

For comparison purposes of the two methods, values are needed for  $D_m$  and  $F_m$ . Using the following values, one obtains

$$D_m = 2.78 \times 10^{-47} \frac{\text{kg}^2 \cdot \text{m}^2}{\text{sec}^3}$$

$$F_m = - 5.27 \times 10^{-20} \text{ nt}$$

$$\text{where } k = 1 \times 10^7 \text{ m}^{-1}$$

$$h = 1.054 \times 10^{-34} \text{ J-sec}$$

$$A = 1 \times 10^8 \text{ sec}^{-1}$$

$$m = 4 \times 10^{-26} \text{ kg}$$

Methods 1 and 2 can now be directly compared to see which has the least stringent requirement on the time increment vs the velocity increment. For method 2, the constant value in 90 is

$$\Delta t < \frac{2D_m}{|F_m|} \approx 2 \times 10^{-8} \text{ sec} \quad \text{Method 2 (95)}$$

For method 1 the calculation is more tedious. A table of values calculated from 88, of  $\Delta v$  vs  $\Delta t$  is given in Table I. This shows that method 1 has a less stringent requirement upon the time increment. So method 1 will be used as the difference equation to solve the Fokker-Planck equation for new values of the velocity distribution function.

#### Analysis of Scanning Frequency Laser Cooling

The theory of using a scanning frequency laser to slow the speed of an atomic beam was developed earlier. A specific case is now analyzed using this theory. Prodan and Phillips (Ref 10 pg 137) report the use of a scanning frequency laser tuned to 589 nm (Ref 22 pg 3826) to slow an atomic beam. The laser is tuned so as to initially interact with atoms at a velocity of 1100 m/sec. The laser is swept at a rate of  $6.4 \times 10^{11}$  Hz per sec. The laser intensity is 5100 watts/m<sup>2</sup> (Ref 23). Experimental results were reported for scans of 480 and 750 MHz. This information will be used to generate a case similar to this so comparisons can be made between theoretical and experimental values.

Several important constants are needed. The Rabi flopping frequency is given in 96.

$$\Omega = \frac{\mu E}{\hbar} = \left[ \frac{b \pi c^2 A I}{\omega_0^3 \hbar} \right]^{1/2} \quad (96)$$

This is because the dipole moment  $\mu$  is

TABLE I

Comparison of  $\Delta U$  vs  $\Delta t$  For Method 1  
Stability and Convergence Requirements

$\Delta U =$ (m/sec)	$\Delta t =$ (sec)
.1	$7.59 \times 10^{-8}$
3.75	$2.85 \times 10^{-7}$
.5	$3.80 \times 10^{-7}$
1.0	$7.59 \times 10^{-7}$
1.5	$1.14 \times 10^{-6}$
2.0	$1.52 \times 10^{-6}$
2.5	$1.90 \times 10^{-6}$
3.0	$2.29 \times 10^{-6}$
3.5	$2.66 \times 10^{-6}$

$$\mu = \left[ \frac{3Ak^3}{4\omega^3} \right]^{1/2}$$

(Ref 13 pg 1086), (97)

and E is

$$E = \left[ \frac{8\pi I}{c} \right]^{1/2} \quad (98)$$

Here, I is the intensity of the laser in watts/m<sup>2</sup>. Using Prodan and Phillips numbers then,  $\omega = 5.5 \times 10^8 \text{ sec}^{-1}$ . This gives a maximum allowable scan rate of  $1.31 \times 10^{13} \text{ sec}^{-2}$  from equation 58. Prodan and Phillips reported a rate of  $4.02 \times 10^{12} \text{ sec}^{-2}$  and  $6.28 \times 10^{12} \text{ sec}^{-2}$ . Both of these are slower than the calculated maximum value. Other needed numbers are

$$k = \frac{2\pi}{\lambda} = 1 \times 10^7 \text{ m}^{-1} \quad (99)$$

$$\omega = ck = 3 \times 10^{15} \text{ sec}^{-1} \quad (100)$$

Table 1 gives acceptable values of the time increment for various values of the velocity increment. If the force and diffusion coefficients are not to change by 1/10 over the step size, then the velocity step must be less than 5 m/sec. A step size of 1.5 m/sec for velocity and  $5 \times 10^{-7}$  sec for time will be used.

The program used to solve the Fokker-Planck equation is given in Appendix I. A brief description of the program will be given here. Figure 1 is a flow chart for the program.

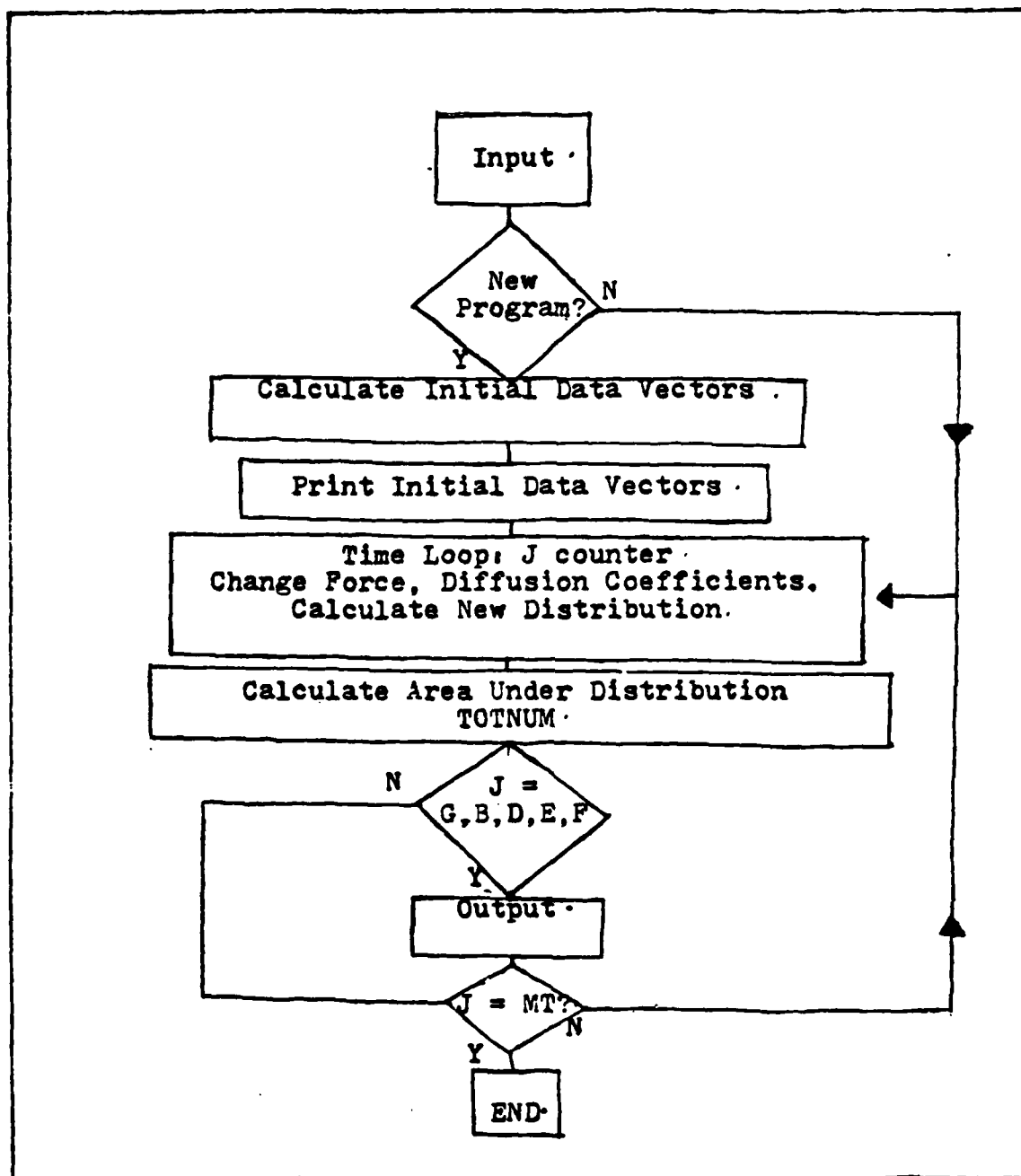


Figure 1. Flowchart for FPLK Program

The program is written in Fortran 77 and was run on the AFIT Vax computer.

The program has three start modes. One exits the program immediately. The second starts the program for the first time, and the third restarts the program if it was broken off in the middle of a run. The program is sometimes terminated before completion because the running time becomes excessive for various combinations of  $\Delta t$ ,  $\Delta v$ , and the rate of de-tuning. When the program is restarted, the data vectors are read back into working memory. These vectors are saved as a routine process within the program. The program then skips directly to the section that solves the Fokker-Planck equation using the data vectors and method 1.

The initial start mode reads in 21 values which characterize the problem. The data vectors are then created. The first data vector is the velocity. It is calculated using a simple summing process and is called VELCTR. The initial velocity distribution function is calculated using equation 101 (Ref 12 pg 20). It is named DFTN.

$$\xi = \frac{v^3}{\alpha^4} \exp \left\{ -\frac{v^2}{\alpha^2} \right\} \quad (101)$$

where  $\alpha = \left[ \frac{2kT}{m} \right]^{\frac{1}{2}}$  and  $v = \text{Velocity (m/sec)}$   
 $k = \text{Boltzmann's constant,}$   
 $T = \text{Temperature } ^\circ K$   
 $m = \text{Mass of atom.}$

The force is computed using equation 49 and is called FORCE. The diffusion coefficient is calculated using equation 50 and is called DIFUSN.

The section that solves the Fokker-Planck equation using difference equation method 1 is the major part of the program. The values for the distribution function are calculated for the next time increment using values at the current time. Thus, the driving mechanism for the program is an iteration loop in time with counter  $J$ . Instead of recomputing the force and diffusion coefficients at each time increment, a interpolation routine is used to shift the values down the velocity axis an amount equal to the amount they move in the time increment. This can be done because the force and diffusion coefficients are represented by a curve dependent on the velocity that is translated to lower velocities as time proceeds. An examination of equations 49 and 50 will convince the reader of this.

The change in the distribution function called DELDFN, is calculated for the  $i$ th velocity and the  $j + 1$ th time using the method 1 difference equation. This change is added to the old value of DFTN and a new (i.e.  $j + 1$ th) distribution function is calculated all along the velocity axis. The area under the distribution function represents the intergral of the curve over all velocity space. Thus, it represents the number of atoms under consideration. This number should remain constant since the number of particles in the beam is a constant. The



value for the area is called TOTNUM and is calculated using a rectangle integration formula.

The results of the calculations are printed into two different files. A table of output values called WRTDAT1, is used as the input to the graphics package. The table has four columns with no headers or other identifying information. The four columns are the VELCTR, DFTN, FORCE and J values respectively. The second output file is called outputx where x is a number that keeps track of the output file number. This file contains the time increment and the value of TOTNUM, as well as the values of velocity, DFTN and FORCE. The outputx and WRTDAT1 files contain values for five different time increments.

It should be noted that the do loop that runs the outputx and WRTDAT1 files, prints every Mth velocity value. This can significantly cut down on the file space required. It does tend to cause losses in the accuracy of the results since the maximum value for the distribution function may be in between the Ith and  $I + M$ th values. If  $M = 1$ , the stability and convergence criteria suggest that the maximum value will be printed for all the values at all the velocities.

The values for TIME and TOTNUM are printed every 100 time iterations. A counter called Q is incremented each time step. When it reaches 100, the data vectors discussed above are stored and the values for TIME and TOTNUM are printed. The value of TOTNUM gives a running check of the stability of the difference equation. If TOTNUM changes significantly, it is a

sure sign that the difference equation is unstable.

To insure that the convergence and stability requirements are met, the program will be rerun with half the step sizes for the velocity and time increments. If the values of FORCE, DFTN, or velocity where the peak of the distribution function sits, change much with respect to their initial amounts, then the step size will be rehalved until it changes no more than 20%. The following is a description of the results for the difference equation for various initial conditions.

If the laser is not swept in frequency, then the force interacts with only one velocity of atoms. Figure 2 shows the initial velocity distribution function for the atoms before the laser is turned on. Figure 3 shows the distribution function after the laser has been turned on for one millisecond. As shown in figure 3, the force causes a narrow spike to appear in the distribution function. The peak is very narrow compared to the initial distribution function. The computer took approximately 950 CPU seconds for this calculation.

If the peak is Gaussian, then the FWHM is related to the  $\sigma$  spread of the peak by 102.

$$\left(\frac{\text{FWHM}}{2}\right)^2 = \sigma^2 2 \ln 2 \quad (102)$$

The  $\sigma$  is the root-mean-square deviation of  $v$  from the mean  $v$  of the Gaussian distribution (Ref 18 pg 24). It therefore provides a direct measure of the width of the distribution

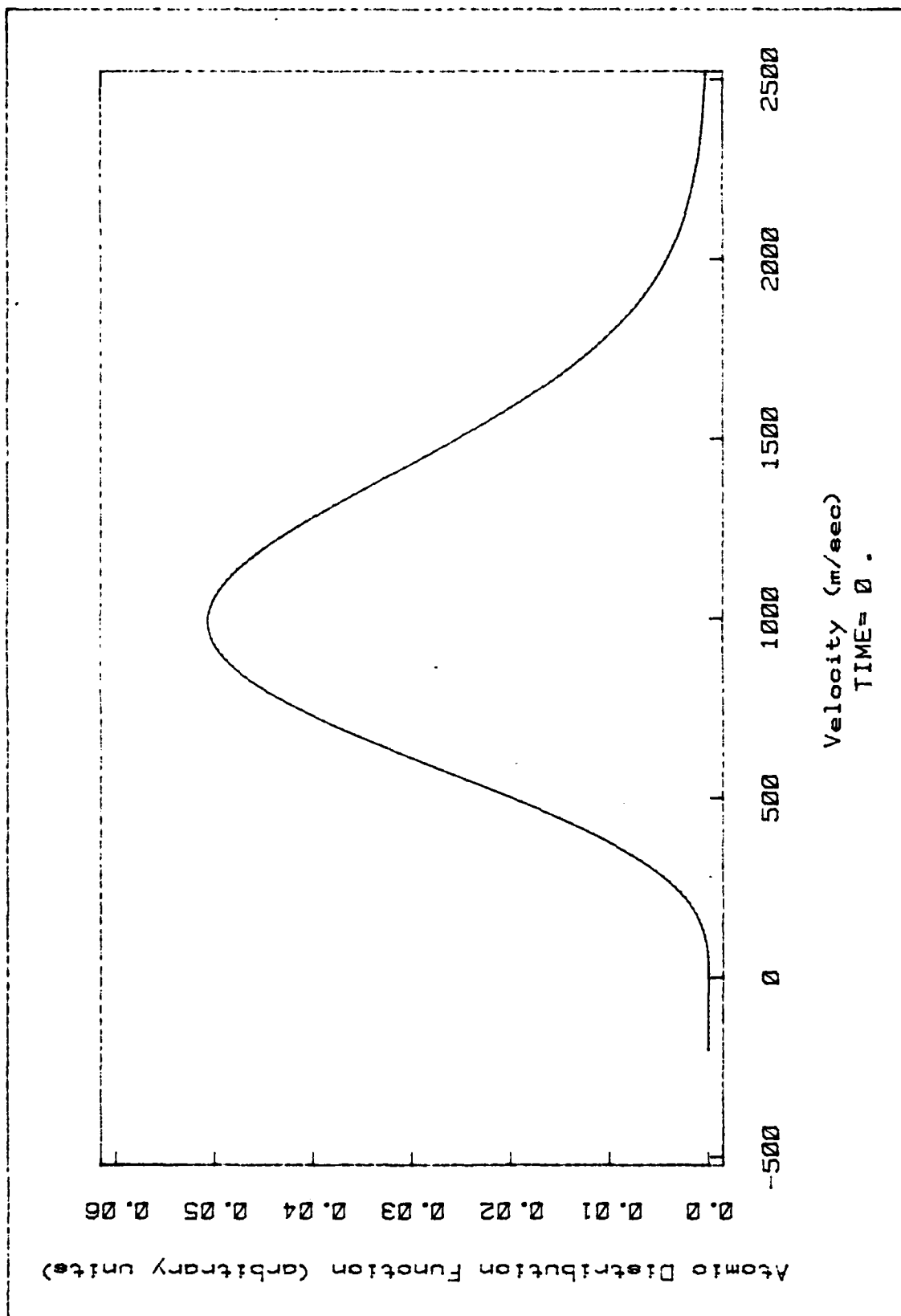


Figure 2. Initial Distribution

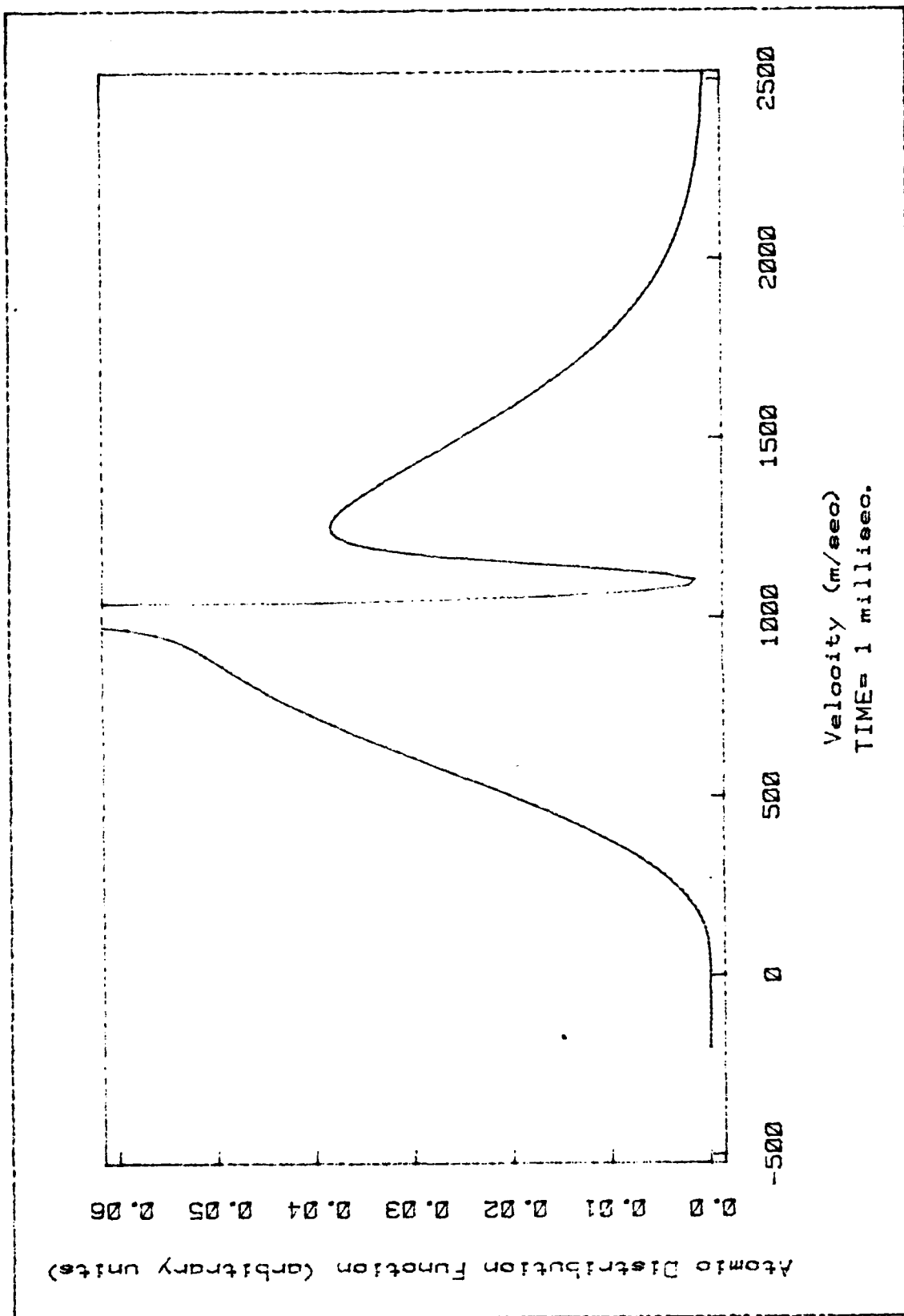


Figure 3. Distribution With No Frequency Scan

function about the mean  $\bar{v}$  (Ref 18 pg 34). The  $\sigma$  is important because it can be related to a characteristic temperature for Gaussian velocity distribution functions.

Following Reif, the  $\sigma$  is related to this temperature by

$$T = \frac{m\sigma^2}{k} = \frac{m \left( \frac{FWHM}{2} \right)^2}{2 \ln 2 \cdot k}, \quad (103)$$

where  $k$  is Boltzmann's constant and  $m$  is the mass of the particles (Ref 18 pg 266). So the narrower the peak in the distribution, the "colder" the temperature of the atoms. Using equation 103, one can compare the initial and final temperature of the atomic beam by knowing the FWHM of the distribution function before and after the laser interacts with the beam. The initial FWHM of the velocity distribution in figure 2 yields a temperature 543.6 °K. The final FWHM of the velocity distribution from figure 3 yields a temperature of  $\sim .2$  °K. As can be seen, the beam is "cooled" by the laser interacting with it. The laser soon moves all the atoms in resonance with it to slower velocities. If the frequency of the laser does not change, the atoms will assume a steady state solution much like that shown in figure 3.

The atoms speed is not slowed appreciably for this case. This is because the force function is very narrow. When the atoms slow by a small amount, they go out of resonance with the laser. To get a feel for how small a change in velocity

this is, look at the FWHM of the force. The FWHM of the force is (Ref 11 pg 226).

$$\text{FWHM} = (A^2 + 2\Omega^2)^{1/2} = 1.41 \times 10^8 \text{ sec}^{-1} . \quad (104)$$

This FWHM has units of radians/sec. In velocity this converts to

$$\Delta v = \frac{\Delta \omega}{k} = 14.1 \text{ m/sec} . \quad (105)$$

Thus, the atoms only have to slow ~15 m/sec and they are out of resonance with the force. This is why the laser frequency must be swept.

To see the effect of the laser frequency sweeping, a case similar to that of Prodan and Phillips will be run. The laser is swept for 480 MHz at a rate of .64 GHz/millisec. This corresponds to a rate of  $4.02 \times 10^{12} \text{ sec}^{-1}$  in radian measure, with a total time of  $7.5 \times 10^{-4} \text{ sec}$ . Figure 4 and 5 give the initial and final positions of the distribution function. As can be seen, the laser sweeps the atoms to a slower overall velocity as well as narrowing the peak. The peak of the distribution function is at a velocity of 740 m/sec. The time and velocity steps have been cut. The step size was halved since the value for the peak of the distribution function changed by 27% after being halved once. This was felt to be large, so the step size was repeatedly halved. This time the

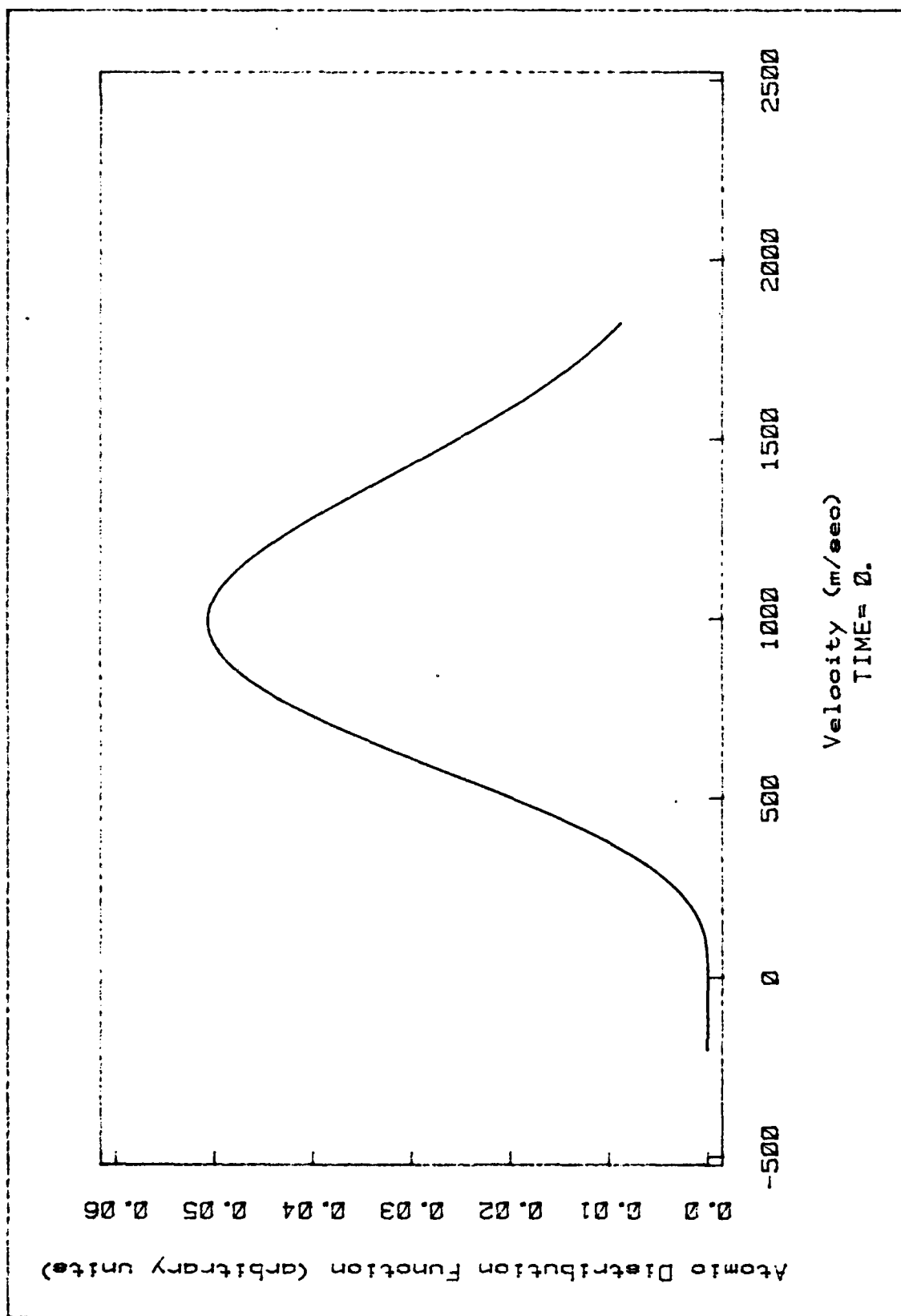


Figure 4. Initial Distribution for  
480 MHz Scan

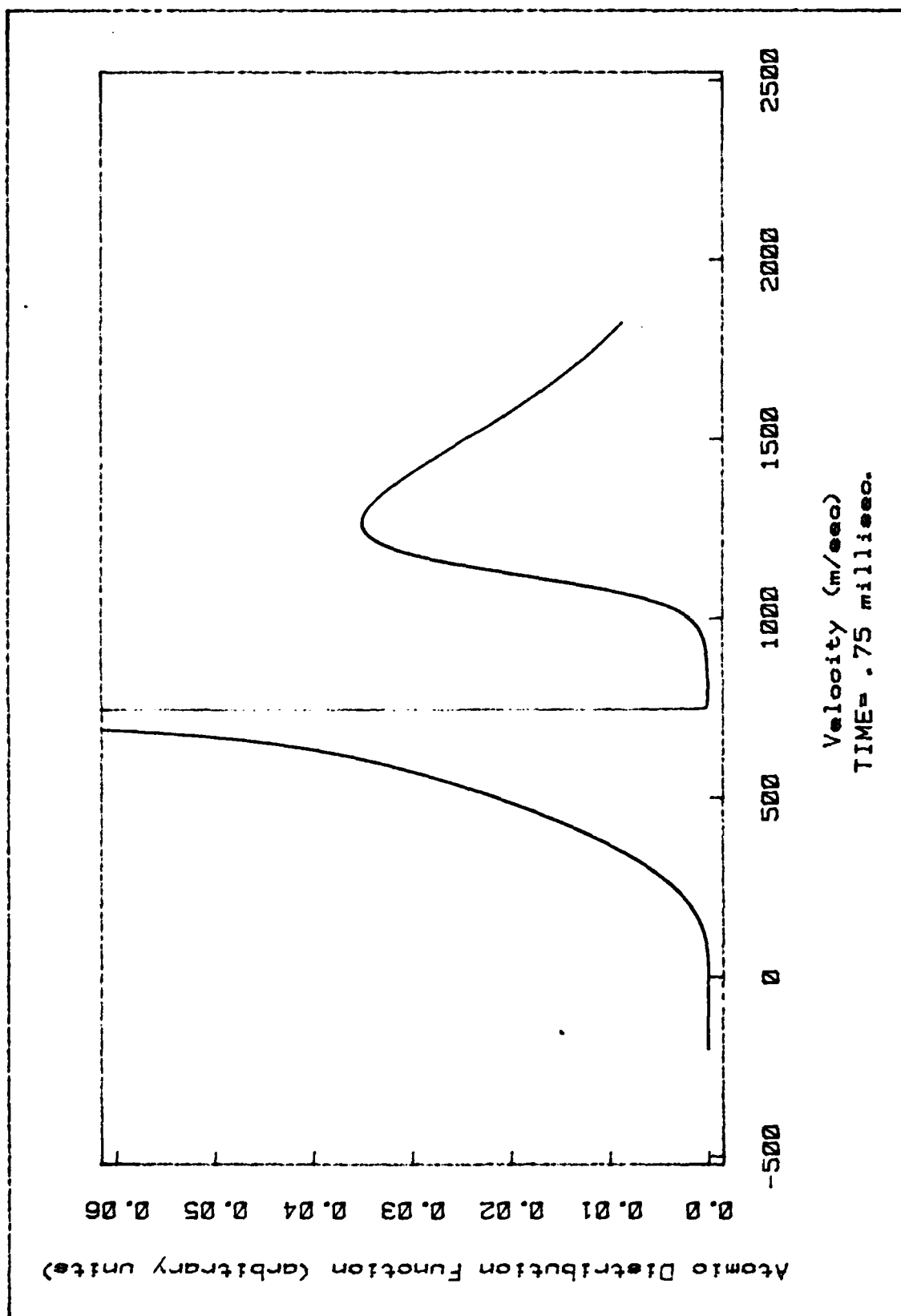


Figure 5. Final Distribution for  
480 MHz Scan



resulting change in the peak of the distribution function was 23%. The FWHM of the narrow peak is 7.03 m/sec. This corresponds to a temperature of  $2.48 \times 10^{-2}$  °K.

Another case experimentally run by Prodan and Phillips was with the laser sweeping 750 MHz at a rate of 1 GHz/millisecond. This corresponds to a rate of  $6.28 \times 10^{12}$  radians/sec<sup>2</sup> and a time of  $7.5 \times 10^{-4}$  sec. Figures 6 and 7 show the results of the difference equation for this case. Again the overall results are the same. The atoms are slowed down and the distribution function becomes very peaked. The FWHM is 6.5 m/sec, which corresponds to a temperature of  $2.122 \times 10^{-2}$  °K. The final peak of the distribution function is at velocity 586.75 m/sec. If the atoms were following the force exactly, theory would expect the final velocity to be 660 m/sec.

An interesting calculation is to see if there exists a lower limit on the translational velocity of the atoms and if there exists a lower temperature bound on that peak. A rate of  $4.02 \times 10^{12}$  sec<sup>-2</sup> was used for a time of  $2.475 \times 10^{-3}$  sec. Figures 8 thru 13 show the atoms slowing down as the laser frequency sweeps down. The calculations show that the translational motion of the atoms can be stopped completely. Indeed, they can be turned around and be made to go the other direction. However, a lower limit is found to the temperature. The smallest FWHM measured from the calculations was 6.25 m/sec. This corresponds to a temperature of  $1.96 \times 10^{-2}$  °K.

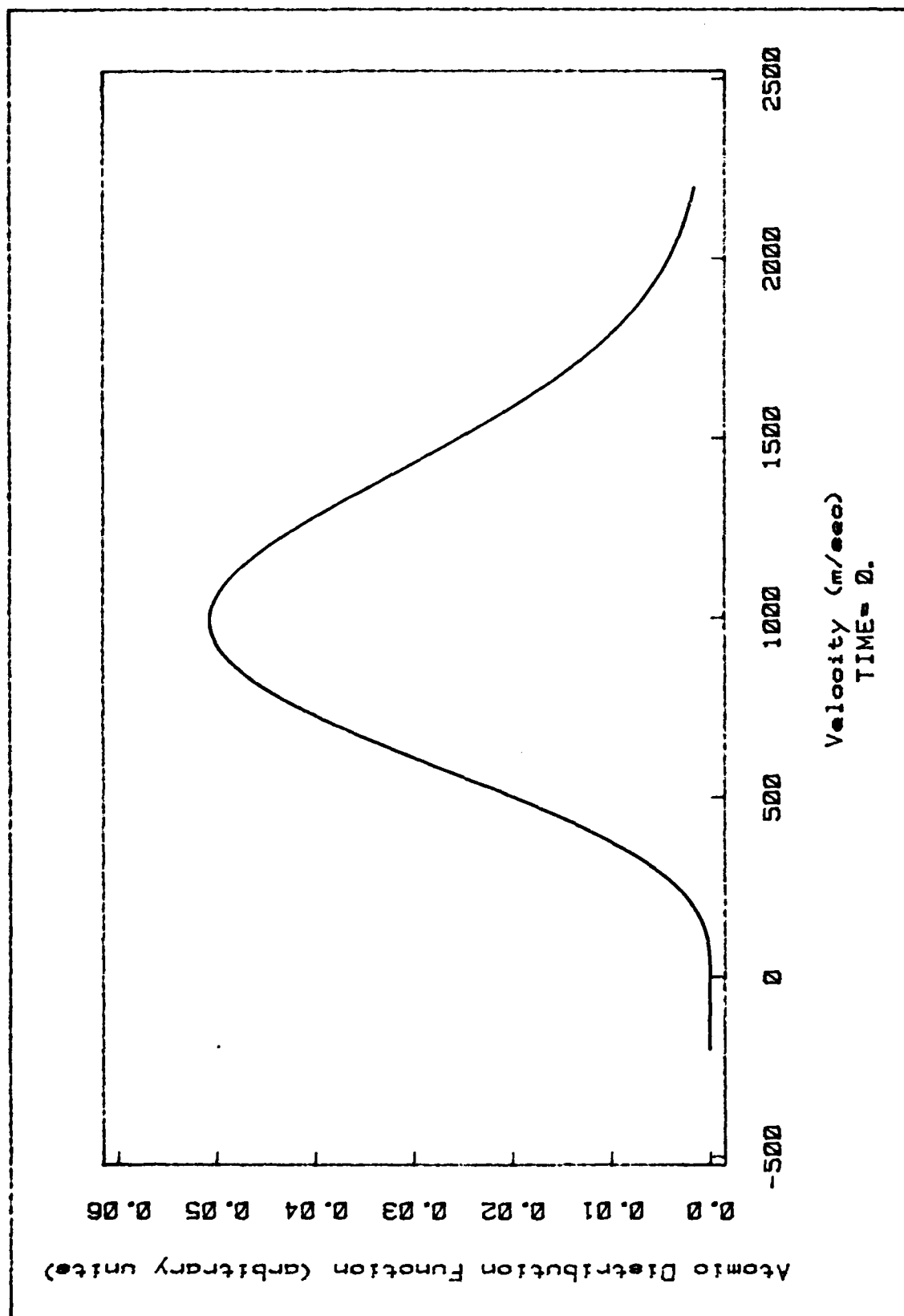
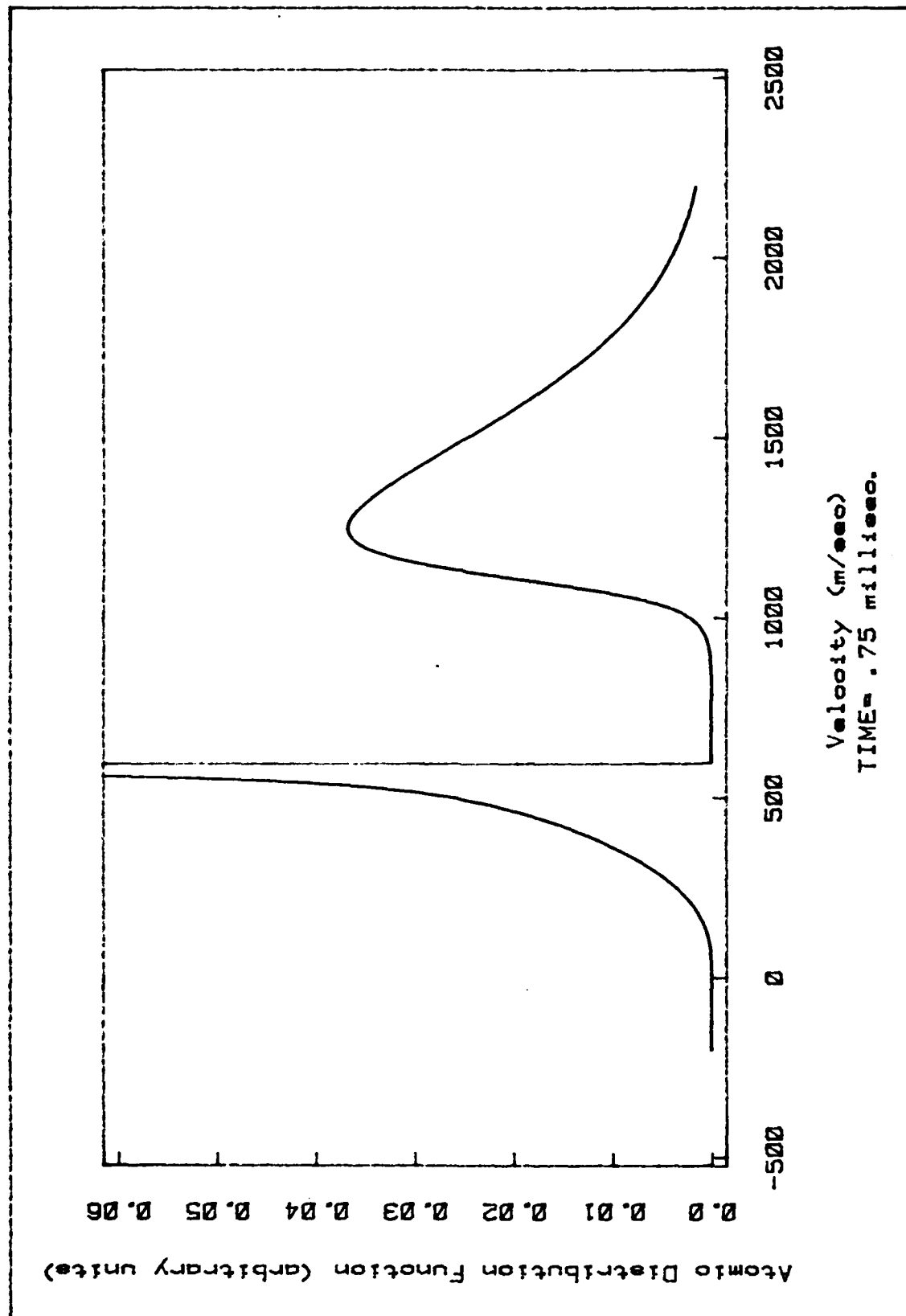


Figure 6. Initial Distribution for  
750 MHz Scan



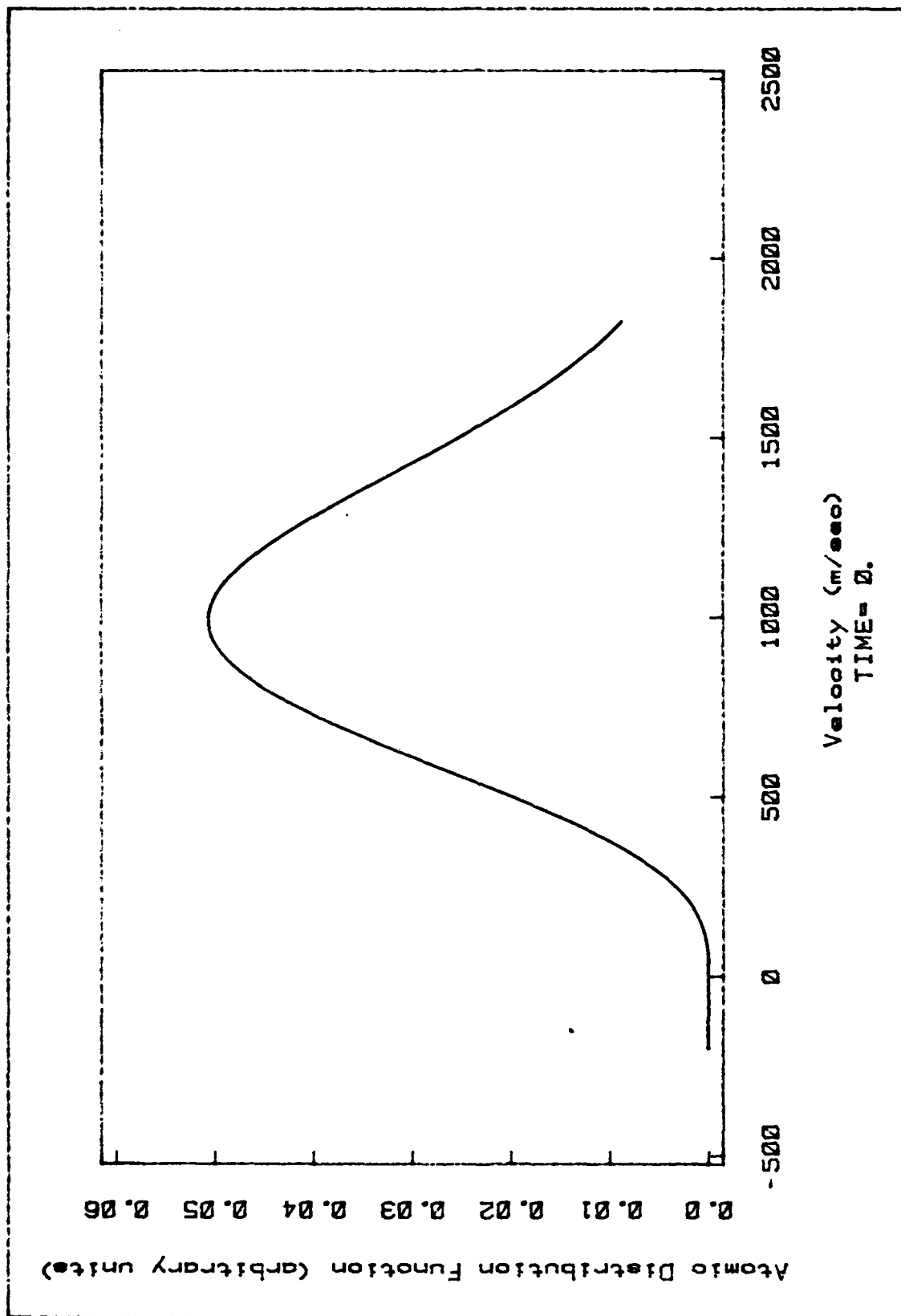


Figure 8. Initial Distribution for  
Maximum Cooling Scan

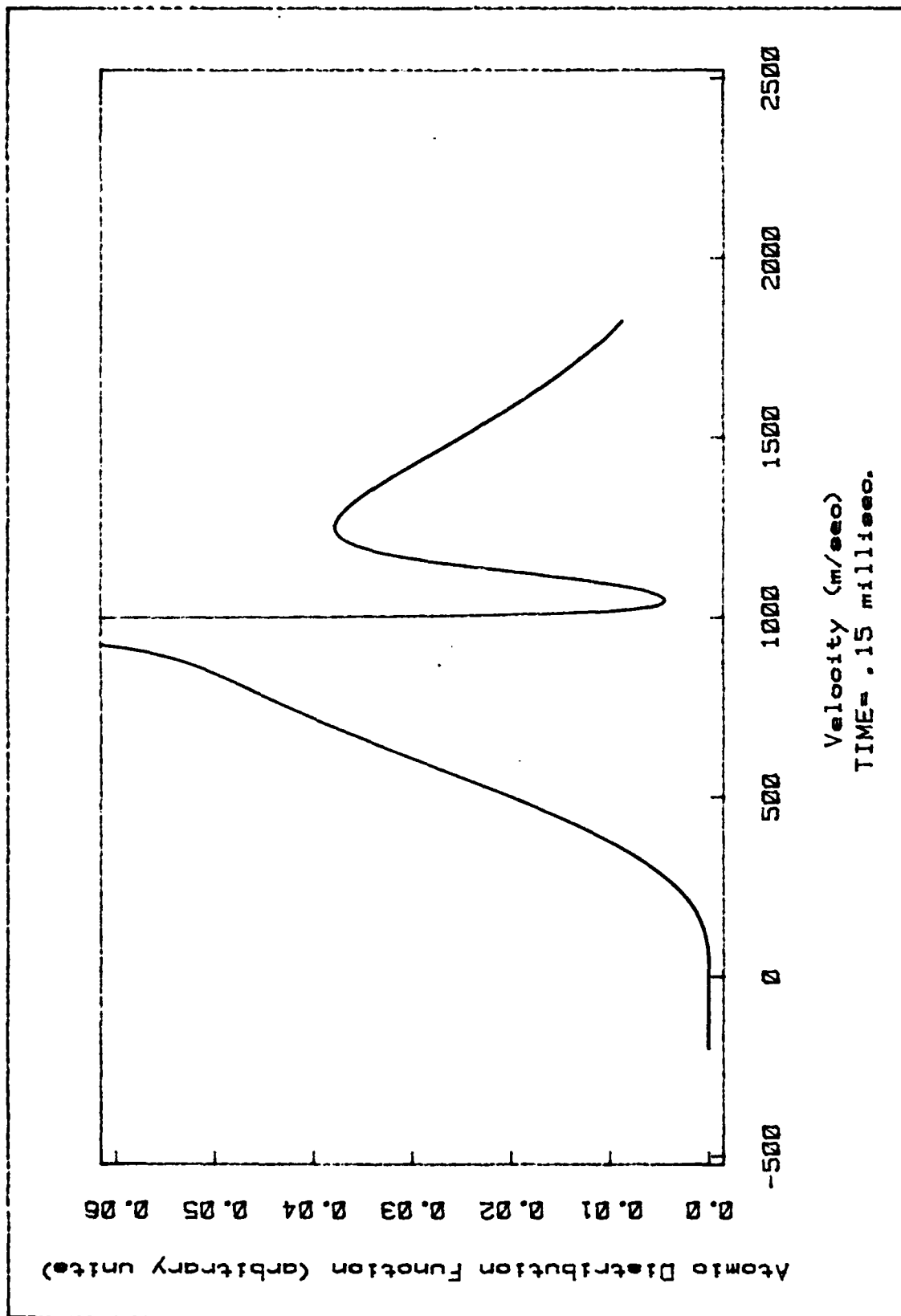


Figure 9. Second Distribution for  
Maximum Cooling Soan

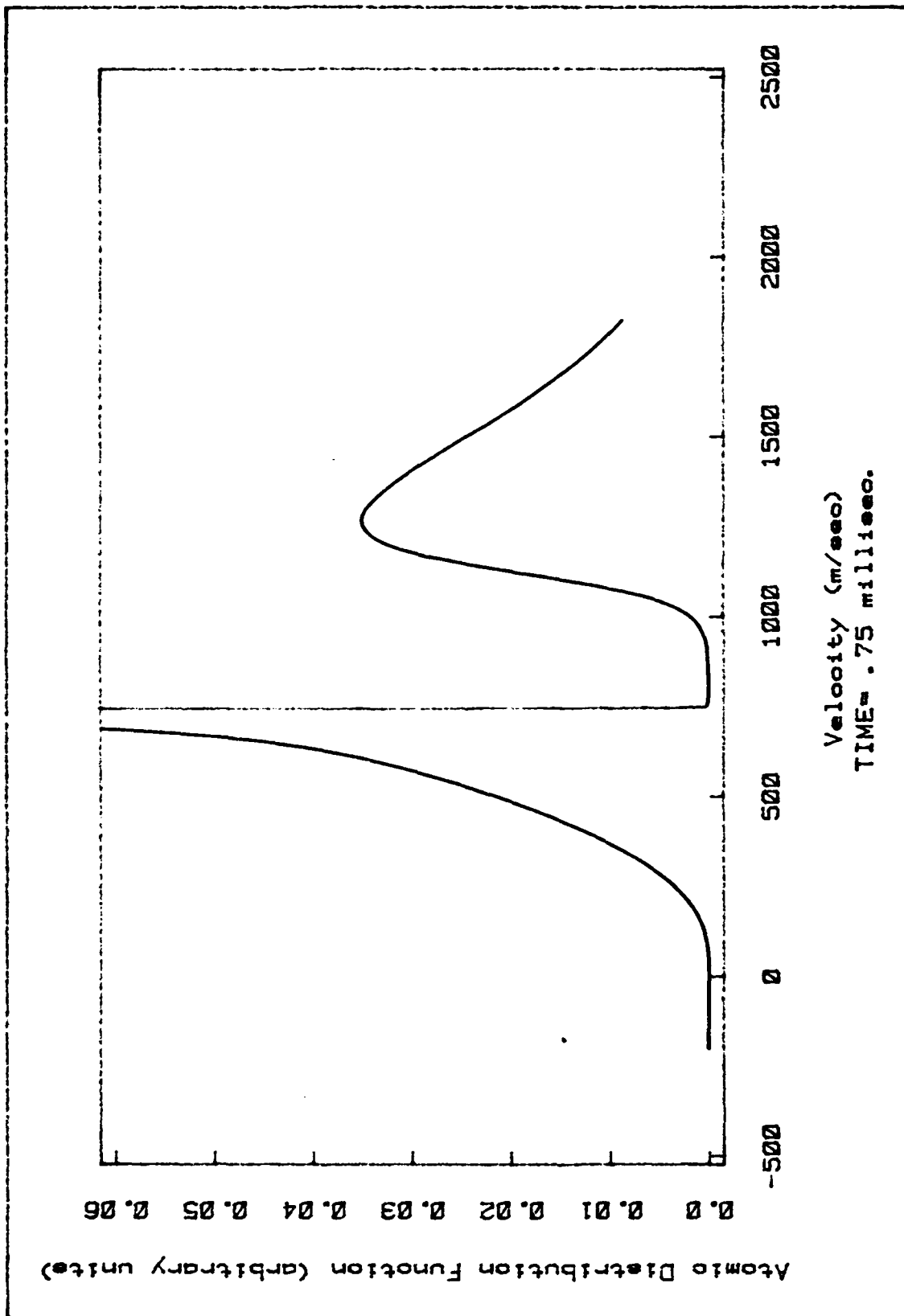


Figure 10. Third Distribution for  
Maximum Cooling Scan

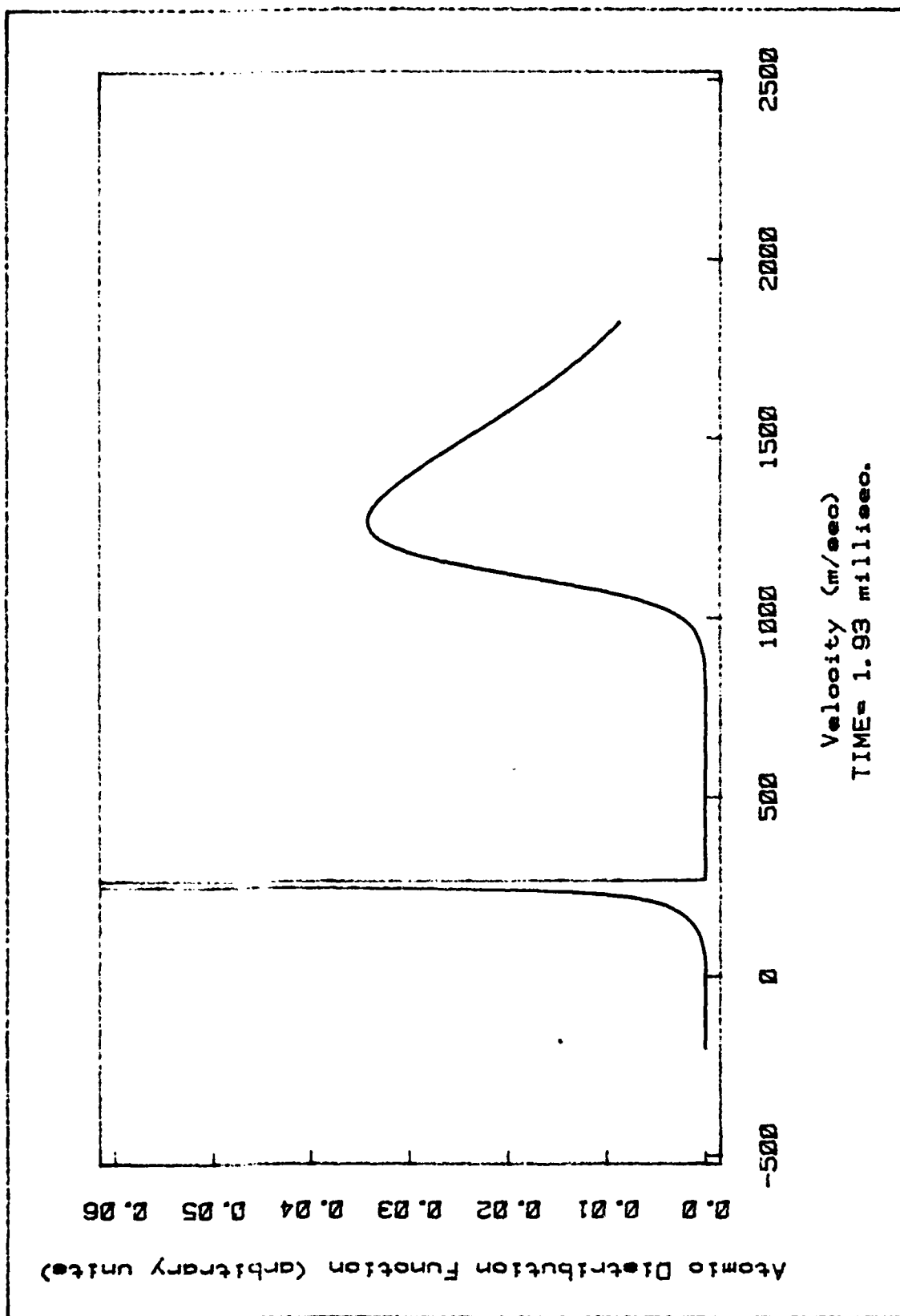


Figure 11. Fourth Distribution for  
Maximum Cooling Scan

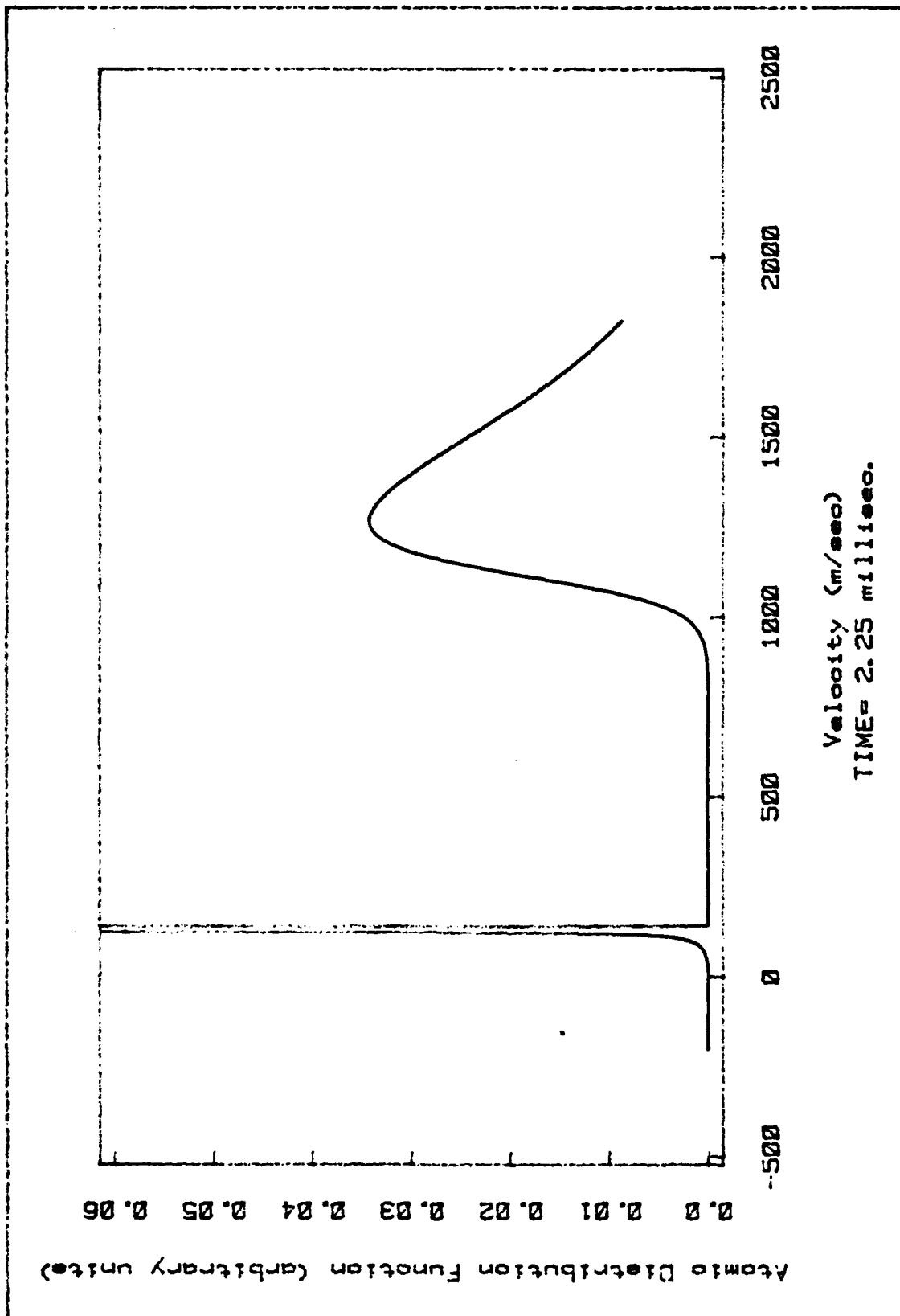


Figure 12. Fifth Distribution for  
Maximum Cooling Scan



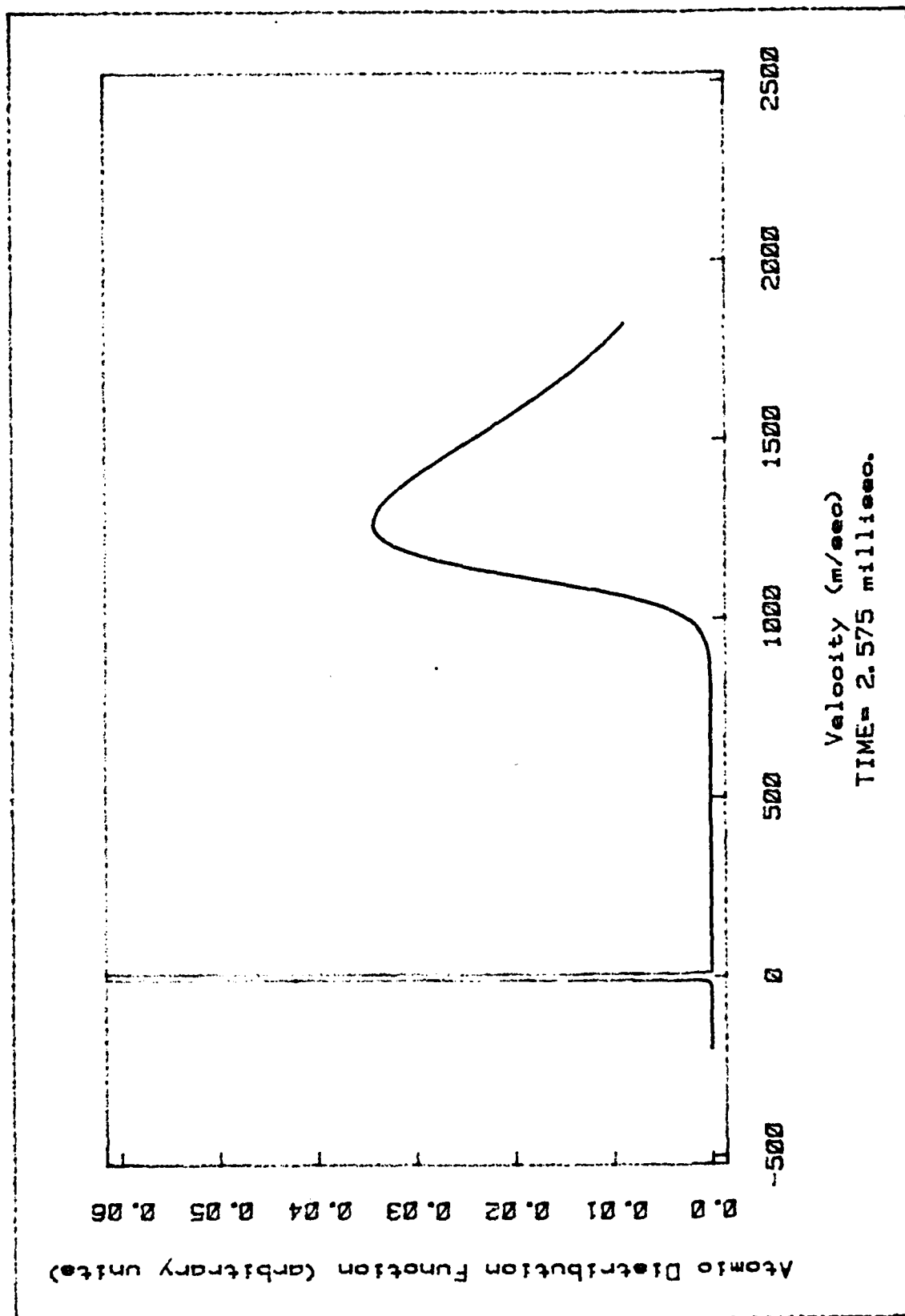


Figure 13. Final Distribution for  
Maximum Cooling Scan

## Discussion

Prodan and Phillips of the National Bureau of Standards have reported experimental results for a similar case to that just analyzed. In that experiment, the laser was focused an amount equal to the divergence of the atomic beam (Ref 23). Thus, the electric field is always perpendicular to the atoms velocity. This was done so as to make the laser look more like a plane wave. Table II summarizes their results and compares them to the results from the analysis performed before. Included in Table II are theoretical calculations for the velocity at which the peak of the velocity distribution function will end. These values are obtained from 106.

$$\Delta v = \frac{\Delta \omega}{k} \quad (106)$$

As can be seen from Table II, the values for the end velocity of the peak agree with the experimental values within 10%. The values for FWHM do not show such agreement. As will be shown later, the gaussian nature of the laser leads to a different force term from that used in the analysis. This different force is analyzed to order of magnitude to see if it should cause changes in the final value of the FWHM. The conclusion at this point is that the gaussian nature of the laser does not make significant changes unless focussed to a very small spot size. Prodan and Phillips do not give experimental error bars for the values of the FWHM (Ref 10 pg 140). Thus it is possible

TABLE II

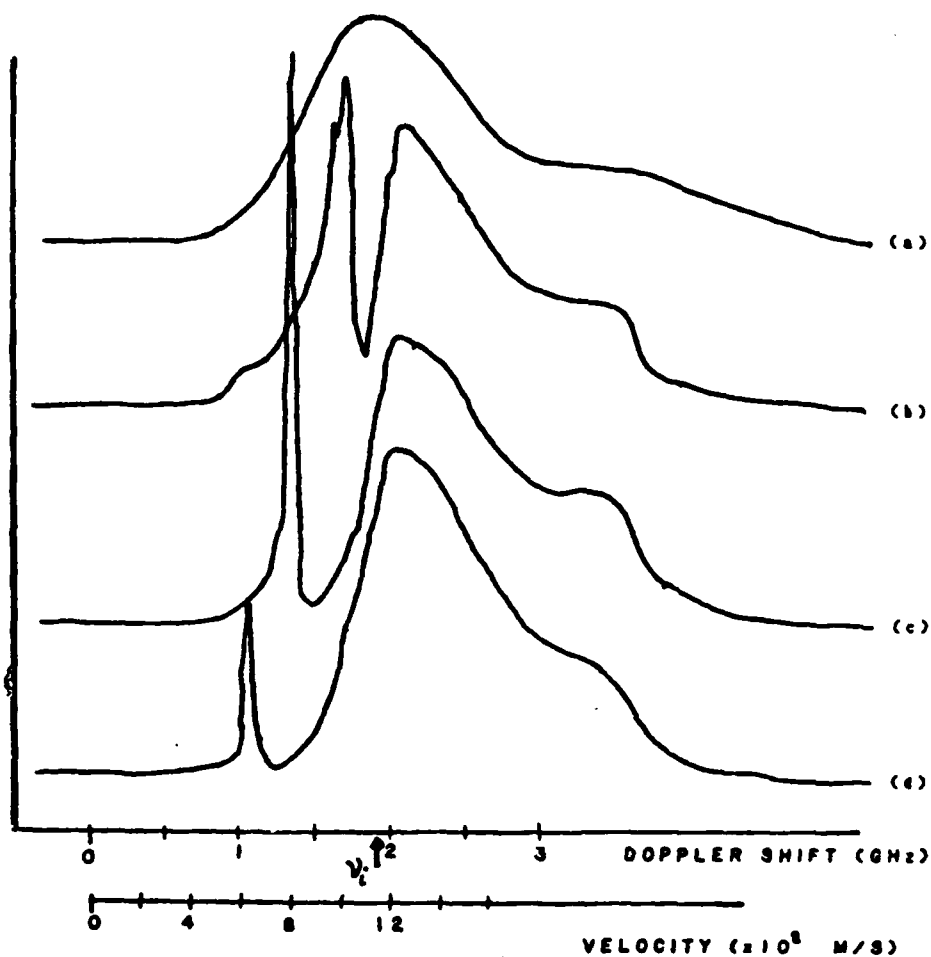
Comparison of Experimental, Numerical and  
Theoretical Values For Swept Frequency Laser Cooling

		Experimental	Numerical	Theoretical
Case 1 480 MHz	Final Velocity for Peak of Dist.	830 m/sec	740 m/sec	820 m/sec
Scan	FWHM For Peak of Dist.	40 m/sec	7.0 m/sec	-
Case 2 750 MHz	Final Velocity for Peak of Dist.	620 m/sec	586 m/sec	660 m/sec
Scan	FWHM For Peak of Dist.	40 m/sec	6.6 m/sec	-

that the factor of six difference between experimental and numerical values for the FWHM is not exceedingly large. Further data is required for a more definite resolution to this discrepancy.

The important consideration is that the numerical calculations predict the overall characteristics of the experiment quite well. Only one major effect seen experimentally is not shown by the numerical calculations. This effect is best seen by looking at figure 14. This is a reproduction of Prodan and Phillips data (Ref 10 pg 139). As can be seen, the values for the peak of the velocity distribution function decrease for a further slowing of the beam. A review of figures 8 thru 13 shows this effect is not seen by the numerical calculations. This is an important consideration since this effect is responsible for current lower limits obtainable experimentally for translational velocity reduction. At this time the discrepancy between experiment and numerical calculation is unresolved. The numerical calculation predicts that the beam can be slowed arbitrarily close to 0 m/sec in translational speed.

As seen in Table II, the values for the FWHM for the two different experimental cases remain nearly constant. This is explained by the fact that Prodan and Phillips ran the 750 MHz sweep at a slightly faster rate than the 480 MHz sweep. This resulted in the interaction time for the laser and atoms being equal for the two cases. For both runs,



Velocity distribution of the atomic beam for the case of (a) cooling laser blocked, (b) cooling laser on but not scanned, (c) cooling laser scanned for 480 MHz, and (d) cooling laser scanned for 750 MHz.

Figure 14. Prodan and Phillips  
Experimental Data (Ref 10 pg 139)

the laser interacted with the atoms for  $7.5 \times 10^{-4}$  sec. This suggests the FWHM is a function of total interaction time. To check this hypothesis, another computer calculation was performed for the 480 MHz sweep. In this case the rate was increased to  $6.28 \times 10^{12}$  sec $^{-1}$ . As can be seen in figures 15 and 16, the final velocity of the peak is at the same value as before. The FWHM of the peak has changed to 6.644 m/sec for this case. This is a reduction in the FWHM of 12.1% from the previous case.

The physical cause of this effect is not yet understood by the author. It does lead to the interesting prediction that for a given frequency sweep, a faster sweep rate will yield narrower FWHM at the end of the interaction.

Cook gives the lowest achievable temperature for the case of a standing wave laser cooling an atomic beam using the dipole force to slow the atoms (Ref 24 pg 979). To within an order of magnitude estimate, similar arguments yield a lowest achievable temperature for the traveling wave case of

$$\frac{1}{2} m \sigma^2 = \hbar A \quad (107)$$

Here the  $\sigma$  is related to the temperature by equation 102. This yields a smallest expected FWHM of

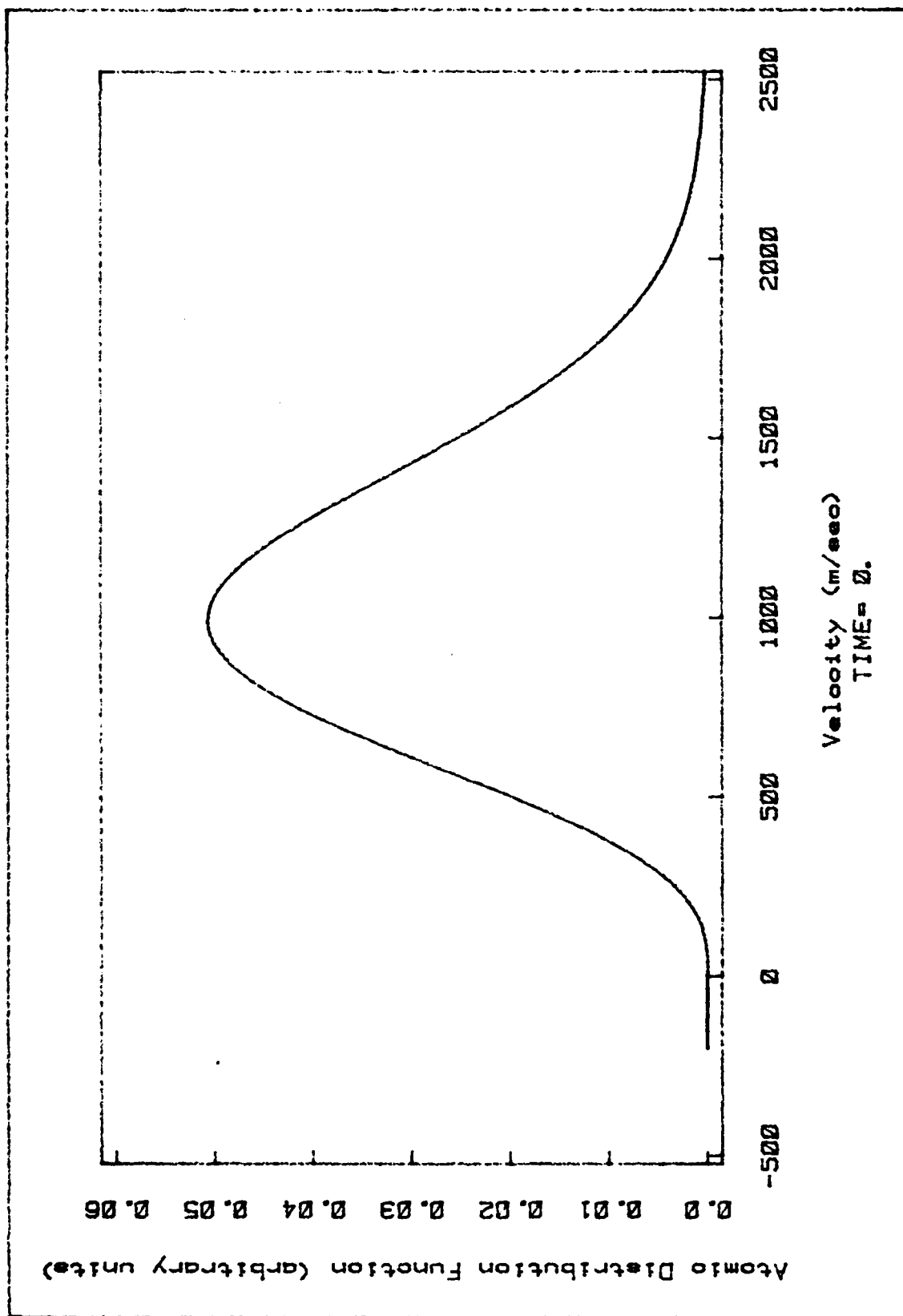
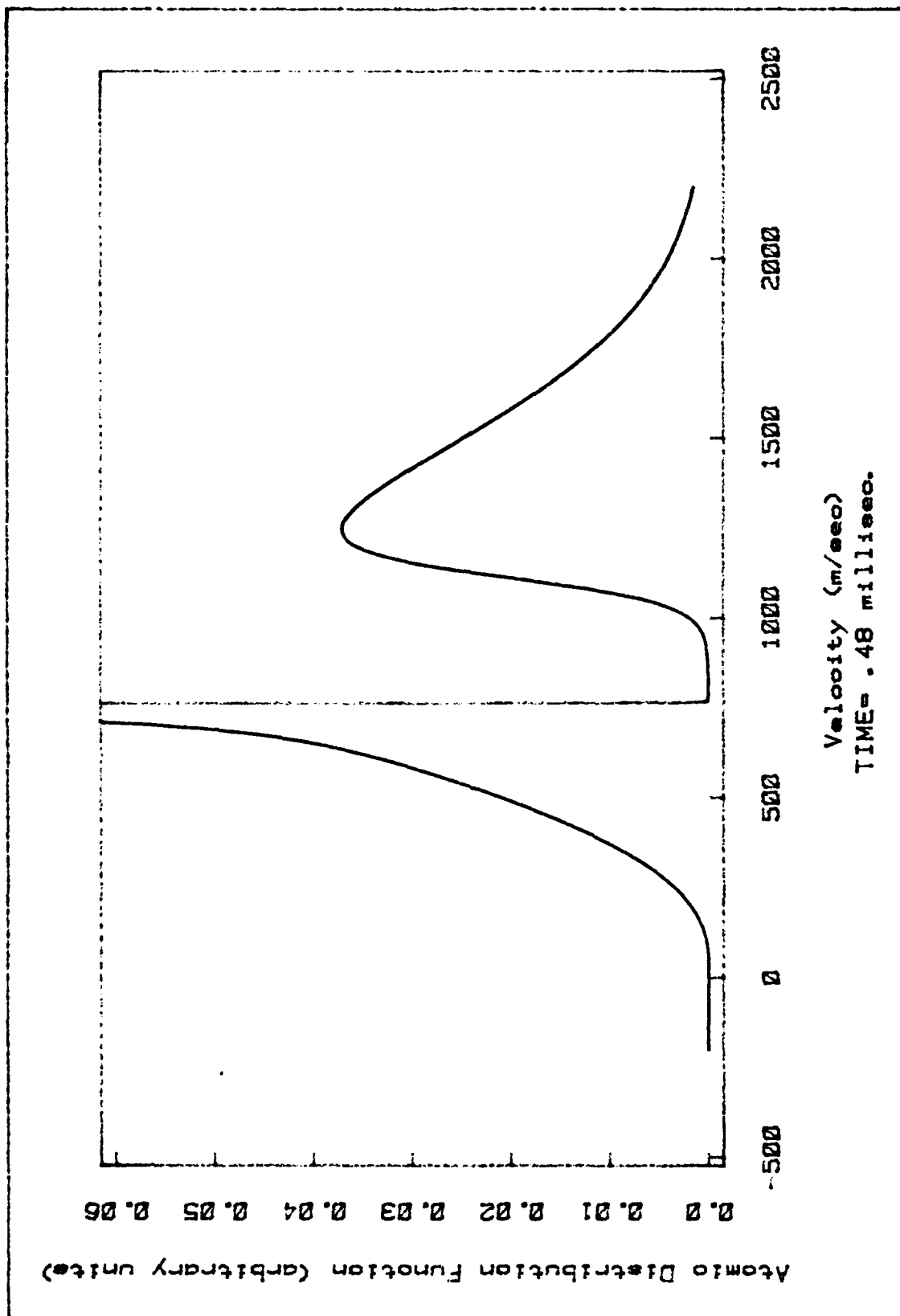


Figure 15. Initial Distribution for 480 MHz  
Accelerated Soan





$$\frac{(\text{FWHM})^2}{2} = \frac{4 \ln 2 A \hbar}{m} \quad (108)$$

The above formula yields a value of the minimum allowable FWHM of about 1.7 m/sec. Table II shows the numerical values of FWHM are in agreement with this calculation in that they do not violate it.

As mentioned before the force induced by a gaussian laser is different from that calculated for an external field in the form of a plane wave. To see this difference the following is presented.

Consider the form of the force in equation 15 evaluated for an external field of a gaussian laser. The field of the laser is presented in equation 109.

$$\mathcal{E}(x,t) = \mathcal{E}_0 \exp \left\{ -\frac{(x^2+y^2)}{\omega_0^2} \right\} \cos(kz - \omega t) \quad (109)$$

Here  $\omega_0$  is the beam waist and

$$\mathcal{A} \text{ is the field strength, } \mathcal{A} = \mathcal{A}_0 \exp \left\{ -\frac{r^2}{\omega_0^2} \right\}, \mathcal{A}_0 = \frac{\mu \mathcal{E}_0}{\hbar}$$

When this is inserted into the force equation, one obtains a translational force the same as before. A transverse force is also present. For on resonance ( $\Delta = 0$ ), the transverse force has the form of equation 110.

$$\vec{F}_{\text{transverse}} = \frac{\hbar k \hat{z} \nabla \mathcal{A}^2}{[4(k\hat{z})^2 + A^2 + 2\mathcal{A}^2]} \quad (110)$$

If the laser is counter propagated to the atomic beam it will defocuss and move the atoms away from the on axis position (Ref 11 pg 20). This is because for a counter propagated laser  $\vec{k} \cdot \vec{r} < 0$ . Thus, since the gradient points inward, the direction of the force is outward. If this force is of the same magnitude as the translational force then the on axis velocity distribution function will have a smaller value. This could change the value for the FWHM. This is a critical question since the numerical values of the FWHM are smaller than the experimental values. To resolve if the gaussian nature of the beam should be neglected a comparison of the relative magnitudes of the translational and transverse forces is performed. For this comparison the maximum value of the transverse force is needed. This is computed much as before. The only difference is that a gradient must be taken of the new Rabi frequency. After this is accomplished one obtains,

$$F_{\text{transvers}} = -\frac{4r\Omega^2(kz)\exp\left\{-\frac{2r^2}{w_0^2}\right\}}{[4(kz)^2 + \pi^2 + 2\Omega^2]w_0^2}$$

The maximum is now calculated noticing that  $kz > A \text{ or } \Omega$ , and that a maximum will occur when  $r=w_0$ . This leads to a maximum transverse force of,

$$F_{\text{transvers, max}} = \frac{\Omega^2 \exp\left\{-\frac{2}{2}\right\}}{kz w_0}$$

Comparison of numerical values with the maximum translational force shows that  $w_0 \approx 10^{-6} \text{ m}$  for the two forces to be equal.

Thus the laser would have to be very focussed for the two forces to be of the same magnitude. This shows that for lasers with a waist of 1 cm the transverse force is negligible. Thus the use of a plane wave for the external field should not affect the FWHM value.

The amount of spread in the peak of the velocity distribution function is a measure of its temperature. If the velocity and the spread in the velocity is small enough, the atoms can be inserted into a trap for neutral atoms. This trap is described by Ashkin (Ref 25). Cook and Hill have a new type of neutral atom trap using the "radiation force exerted by the thin evanescent wave that is generated on the surface of a dielectric medium when laser light is totally reflected internally at that surface" (Ref 26 pg 258). The requirement on the translational speed for both these traps are  $\sim 5$  m/sec. Using a one dimensional analysis there seems to be no reason why these requirements cannot be met.

A discussion of the amount of confidence warranted in the numerical calculations is now in order. The stability and convergence analysis govern the step size for time and velocity. To meet the smooth field approximation, and hence the condition for local stability, the step size of velocity was limited to less than 4 m/sec. After the calculations are performed, the step sizes are halved to see if there are any changes in the answers. When this is accomplished, it is found that changes made independently

for the time increment, do not effect the results as long as the time increment is less than its maximum allowed by equation 96. Changes in the velocity step size are found to effect the answers. This indicates that the stability of the numerical calculations are assured but that some question convergence of the answers to real solutions due to truncation errors still exist.

To investigate the convergence question, the 480 MHz sweep was rerun several times with halved velocity step sizes. In each case the time step size was halved along with the velocity step size. The time step size was checked to insure that it was in accordance with equation 88. The time step size was independently varied to insure that the only changes seen were due to the change in the velocity step size. Table III summarizes the results of this investigation. Included are times that the computer took to run the case. As can be seen, the run times quickly become very long. Most values are not affected by changes in the velocity step size. The value most sensitive to the step size is the peak value of the velocity distribution function. Table III shows the percentage change from one step size to the next for this value. The smallest change seen was 23%. All other values show percentage changes that are smaller. These small changes, along with long run times at small step sizes, convinced the author that acceptable limits of numerical accuracy have been reached at  $\Delta v = .375 \text{ m/sec}$  and  $\Delta t = 1.25 \times 10^{-7} \text{ sec}$ .

TABLE III

Effect of Halving Velocity Increment on Numerical Results

$\Delta V$ (m/sec)	Peak Value of Velocity Dist.	Final Position For Peak Dist.	% change in Peak Value @ $\frac{1}{2}\Delta V$	Run Time (CPU hrs.)
1.5	1.177	734 m/sec	27%	.32
.75	1.614	736 m/sec	23%	.72
.375	2.111	738 m/sec	23%	2.5
.1875	2.755	739 m/sec	-	8.7

The changes in the answers are attributed to truncation errors. The FWHM of the force function is  $\sim 14$  m/sec. With a step size of 1.5 m/sec there are only about nine velocity steps within this FWHM. This causes truncation errors due to the coarse nature of the force function. The stability of the calculations insures that these errors do not propagate and cause the results to wildly diverge. However, the errors are slow to converge, and so affect the final results. As the velocity step size is reduced, the calculated answers converge to the real solutions. A similar argument holds for the peak of the velocity distribution function. The peak becomes very narrow as the atoms slow down. Thus, small velocity step sizes must be used so enough sample points are obtained for the peak. Too large a velocity step size will cause the peak to not have enough sample points. Thus errors will be created in the calculations unless the velocity step size is small enough. Small enough will be defined as there being 20 points under the narrowest function.

The final choice for the velocity step size is .375 m/sec. The time step size is  $1.25 \times 10^{-7}$  sec. This time step size is in agreement with equation 88. This velocity step size is used since it provides  $\sim 20$  points under the narrowest function. The narrowest function, and the function most sensitive to changes in the velocity step size, is the peak of the velocity distribution function. It changes by 23%

when the velocity step size is changed by halving it. If this change is neglected then all numerical results agree with the experimental results within 10%. Neglecting the change in the peak of the velocity distribution function is allowable since it is only important if the peak decreases as the atoms are slowed. Since changes in the velocity step size always increase the peak value of the velocity distribution function, neglecting it for purposes of determining accuracy is acceptable.

The important parts of this discussion are now summarized. The numerical results agree with the experimental results to within 10% for all values except for the FWHM and the peak of the distribution function. These two values are very sensitive to changes in velocity step size because of truncation error. For a step size indicated before the FWHM are believed to be correct to 15%. The minimum FWHM observed numerically agree with a calculation for the minimum allowable FWHM. The gaussian nature of the laser is shown not to effect the FWHM as long as the laser is not focussed to micron size. The numerical calculations give rise to the prediction that for a given amount of frequency change, a faster sweep rate produces a narrower FWHM.

## IV Conclusions and Recommendations

### Review of Major Results

Ehrenfests theorem, along with an assumed form of the external electromagnetic field, yields the set of coupled differential equations 7 thru 10. These equations give the interaction force between the laser and the atoms. The internal dynamics of the atom is described by the optical-Bloch equations 8 thru 10. This set of equations are consistent with a more general set of equations that are developed by Cook (Ref 13 pg 1087).

In the smooth field approximation, the set of equations condenses to a single partial differential equation known as the Fokker-Planck equation. This equation is the basis for the analysis performed in this thesis. Along with the Fokker-Planck equation, coefficients are developed for the force and diffusion terms. These are presented in equations 15 and 29 respectively.

The Fokker-Planck equation is rewritten as a difference equation to allow numerical solutions to be obtained. Several difference equations are analyzed using convergence and stability criteria. Equation 60 is selected as the difference equation of choice because it has the least stringent requirements on the step size for time and velocity.

This difference equation is used to analyze the Fokker-Planck equation for a one dimensional geometry. A plane wave laser is incident upon a one dimensional beam.



The laser frequency is swept at a rate given by equation 58. This sweeping brings different velocity atoms into resonance with the laser. The laser imparts quanta of momentum to the atoms and thus slows them down. The atomic velocity distribution function reflects this slowing of atoms by changing from a thermal distribution to a sharply peaked distribution. In general terms, the peak of this distribution follows the laser frequency and slows to low translational velocities, with corresponding narrow spreads in the peak.

This analysis predicts that the translational velocities can be brought arbitrarily close to 0 m/sec. The minimum FWHM of the peak in the distribution function is 6.25 m/sec. This corresponds to a temperature of  $1.96 \times 10^{-3}$  °K, assuming the peak of the distribution function relaxes to a Gaussian distribution. This temperature is a measure of the spread in energy of the atoms within this slow peak. It is also a direct measure of the width of the peak. The minimum FWHM agrees with a limit developed by Cook for the smallest allowable FWHM.

The numerical calculations suffer from truncation error unless the velocity step size is small enough. Small enough is defined as there being 20 velocity points on the narrowest peak in the calculations. The narrowest peak is the distribution function after being cooled by the laser. The value of the maximum of this peak is the value most sensitive to changes in the velocity step size. A velocity step size of .1875 m/sec gives good results but the run time on the computer

is 8.7 CPU hours. This run time is clearly excessive. Thus, a velocity step size of .375 m/sec, and a time step size of  $1.25 \times 10^{-7}$  sec are used. This results in run times of 2.5 CPU hours. The numerical results are believed to be correct to within 10% for these step sizes.

### Conclusions

The Fokker-Planck equation is a powerful tool to study the effects of resonant radiation upon atoms. All effects experimentally observed except one are predicted using a simple one dimensional analysis of the problem. The one dimensional model predicts that the atoms can be brought arbitrarily close to 0 m/sec in translational speed. Although truncation errors force a small velocity step size, and hence long run times, the overall method is still useful. The Fokker-Planck analysis predicts that for fixed frequency sweeps, a faster sweep rate will yield narrower FWHM at the end of the interaction.

The Fokker-Planck equation can be used for analysis of other types of resonant radiation interaction between atoms and photons. The standing wave laser used as an atomic trap is a good example. As long as the atoms enter the trap at slow velocities, the Fokker-Planck equation adequately describes their motion.

In cases where the smooth field approximation is violated, the Fokker-Planck equation should be replaced by the quasiclassical equations developed by Cook (Ref 13 pg 1087).

AD-A163 954

LASER COOLING OF NEUTRAL ATOMS(U) AIR FORCE INST OF  
TECH WRIGHT-PATTERSON AFB OH SCHOOL OF ENGINEERING  
N G MCHARG DEC 83 AFIT/GEP/PH/83D-6

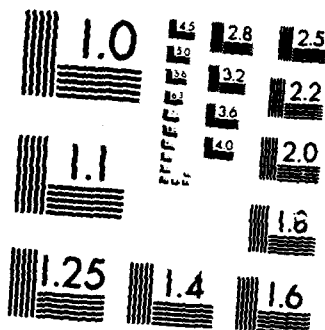
272

UNCLASSIFIED

F/G 20/8

NL





MICROCOPY RESOLUTION TEST CHART  
NATIONAL BUREAU OF STANDARDS-1963-A

An example of this case is found in the optical Stern-Gerlach effect. Due to the quantized nature of the electric dipole moment, the atomic distribution function will be split in half by oppositely directed forces. The Fokker-Planck equation does not yield this result because inherent in its derivation is the assumption that the wave packet under consideration is small compared to changes in the external field.

### Recommendations

Further work in the area of numerical analysis of resonant radiation can be accomplished in at least three different areas. No doubt other interesting applications are present, but these three seem the most obvious or potentially useful to the author.

The Fokker-Planck equation should be used to analyze the standing wave laser used as a neutral atom trap. Such a trap was proposed by Ashkin in 1978 (Ref 26). This type of trap will allow doppler free spectroscopy to be performed upon the atoms inside. The nature of the Fokker-Planck equation reverts to its general form, as in equation 112.

$$\frac{\partial S}{\partial t} = -\frac{p}{m} \frac{\partial S}{\partial x} - \frac{\partial}{\partial p} (F S) + \frac{\partial^2}{\partial p^2} (D S) \quad (112)$$

The force will be given by equation 113 (Ref 13 pg 1089)

$$F^i = \frac{-\hbar \Delta \frac{\partial \Omega^2}{\partial x^i}}{4\Delta^2 + A^2 + 2\Omega^2} \quad (113)$$

The diffusion coefficient is

$$D_t = \frac{\hbar^2 A \Omega^2 \hbar^2}{10(4\Delta^2 + A^2 + 2\Omega^2)} + \frac{\hbar^2 (\nabla \Omega)^2}{2A(4\Delta^2 + A^2 + 2\Omega^2)} \left[ A^2 + 2\Omega^2 - \frac{8\Delta^2 \Omega^2 [4\Delta^2 + 5A^2 + 4\Omega^2]}{(4\Delta^2 + A^2 + 2\Omega^2)^2} \right] \quad (114)$$

The Fokker-Planck equation should be analyzed in two dimensions for the case under consideration in this thesis. The form of the external field is changed to a Gaussian beam, as in equation 109. The force is then given by equations 49 and 110. This analysis may allow determination of the cause of the observed decrease in the peak of the distribution function as the beam is slowed.

The third area also analyzes a Gaussian laser interacting with an atomic beam. In this case the laser is used to sense the position of a neutral beam. The laser is directed towards the neutral beam from the side. The atoms will be resonant with the laser for only a small angle of deflection from the normal. The effect of the laser on the emittance, and hence divergence, of the neutral beam would be of interest to accelerator designers. Cooks quasiclassical equation would have to be solved since the interaction time is very short.

### Bibliography

1. Einstein, A. "On The Quantum Theory Of Radiation," Physik. Zeitschr., 18: 121-128 (1917).
2. Frisch, R. "Experimental Detection of the Einstein Recoil Radiation," Physik. Zeitschr., 86: 42-48 (1933)
3. Hansch, T.W. and A.L. Schawlow. "Cooling of Gases By Laser Radiation," Optics Communications, 13: 68-69 (January 1975).
4. Stein, S.R. "The Design of Atomic Frequency Standards and Their Performance in Specific Applications," in Laser Cooled and Trapped Atoms, edited by William D. Phillips. Washington, D.C.: National Bureau of Standards Special Publication 653, June 1983.
5. Lewis, Lindon "Limitations of Atomic Beam Frequency Standards," in Laser Cooled and Trapped Atoms, edited by William D. Phillips. Washington, D.C.: National Bureau of Standards Special Publication 653, June 1983.
6. Letokhov, V.S. and V.G. Minogin. "Laser Radiation Pressure on Free Atoms," Physics Reports, 73: 1-65 (July 1981).
7. Ashkin, A. and J.P. Gordon. "Cooling and Trapping of Atoms by Resonance Radiation Pressure," Optics Letters, 4: 161-163 (June 1979).
8. Balykin, V.I., V.S. Letokhov, and V.I. Mishin. "Radiative Redistribution of the Velocities of Sodium Atoms by Resonance Laser Radiation," Soviet Physics Journal of Experimental and Technical Physics, 53: 919-924 (May 1981).
9. Prodan, John V., William D. Phillips, and Harold Metcalf. "Laser Production of a Very Slow Monoenergetic Atomic Beam," Physics Review Letters, 49: 1149-1153 (18 October 1982).
10. Prodan, John V., and William D. Phillips, "Chirping the Light -- Fantastic?," in Laser Cooled and Trapped Atoms, Edited by William D. Phillips. Washington, D.C.: National Bureau of Standards Special Publication 653, June 1983.
11. Cook, R.J. "Atomic Motion in Resonant Radiation : An Application of Ehrenfests Theorem," Physical Review A, 20: 224-228 (July 1979).

12. Ramsey, Norman F. Molecular Beams. Oxford: Clacedon Press, 1956.
13. Cook, R.J. "Theory of Resonance-Radiation Pressure," Physical Review A, 22: 1078-1098 (September 1980).
14. Gerald, Curtis F. Applied Numerical Analysis. Reading Massachusetts: Addison-Wesley Publishing Company, 1970.
15. Schiff, Leonard I. Quantum Mechanics (Third Edition). New York: McGraw-Hill Book Company, 1955.
16. Allen, J. and J.H. Eberly. Optical Resonance And Two-Level Atoms. New York: Wiley-Interscience, 1975.
17. Louisell, W.H. Quantum Statistical Properties of Radiation. New York: Wiley, 1973, pg 347.
18. Reif, F. Fundamentals of Statistical and Thermal Physics. New York: McGraw-Hill Book Company, 1965.
19. Churchill, Ruel V. and James Ward Brown. Fourier Series and Boundary Value Problems. New York: McGraw-Hill Book Company, 1978.
20. Kittel, C. Quantum Theory of Solids. New York: John Wiley & Sons, Incorporated, 1963.
21. Roache, Patrick J. Computational Fluid Dynamics. Albuquerque New Mexico: Hermosa Publications, 1972.
22. Phillips, William D. "Rapid Frequency Scanning of Ring Dye Lasers," Applied Optics, 20: 3826-3827 (15 November 1981).
23. Prodan, John V. Personal Telephone Conversation. The laser is initially two centimeters in diameter. It is focused to one millimeter diameter beyond the interaction length. The laser is focused so it matches the atomic beams divergence. This is to make the laser look more like a plane wave. Average values are, .5 cm diameter beam with 100 milliwatts power. National Bureau of Standards, Washington, D.C. 20234, (30 September 1983).
24. Cook, R.J. "Quantum-Mechanical Fluctuations of the Resonance Radiation Force," Physical Review Letters, 44: 976-979 (14 April 1980).
25. Cook, R.J. and Richard K. Hill, "An Electromagnetic Mirror For Neutral Atoms," Optics Communications, 43: 258-260 (15 October 1982).



26. Ashkin, A. "Trapping of Atoms by Resonance Radiation Pressure," Physical Review Letters, 40: 729-732 (20 March 1978).
27. Becker, Richard A. and John M. Chambers, S A Language and System for Data Analysis. Bell Laboratories, 1981.

### Appendix: The FPLK Program

The FPLK program is used to solve the difference equation form of the Fokker-Planck equation. The program is developed to allow maximum flexibility in terms on analyzing different problems. This is accomplished using a large initial data input section. The program is based on a one dimensional analysis described in detail in Section III. The program is written in ANSI standard Fortran 77.

The input data section requires that the operator of the program input 21 values that describe the problem to be analyzed. All inputted values are in the MKS system of units. Figure 17 shows a typical set of input values which were used to analyze the 480 MHz sweep discussed in the Analysis section. Included in figure 17 are lettered captions on the input values, and a key that gives a description of the value and its units.

Once the input data section is mastered, almost any problem can be analyzed using the program. Stability and convergence criteria limit the step sizes for  $\Delta t$  and  $\Delta v$ . The rate of detuning must conform to equation 58.

The CPU time required to run the program becomes excessive as  $\Delta t$  and  $\Delta v$  become small. This is illustrated in table III, which gives run times for various cases. To improve execution speed, several modifications were made to the program. The listing given in the end of this

A	B	C	D	E	F	G	H	I	J
4E-26,	1.25E-7,	.375,	200.,	5.5E8,	950.,	1E7,	3840,	6.28E12,	6400
K	L								
0,	1								
M	N	O	P						
1100.,	1,	1E8,	3E15						
		Q							
		900.	1000.	2000.	3000.	3840			

- A. Mass of the atoms in kg.
- B. Time increment step size in sec.
- C. Velocity increment step size in m/sec.
- D. Value on negative velocity axis where the calculations begin.
- E. Rabi frequency in radians/sec.
- F. Temperature of atomic oven in °K.
- G. Magnitude of wave vector.  $2\pi/\text{wavelength}$ . Units of  $\text{m}^{-1}$ .
- H. Number of time iterations performed.
- I. Detuning rate for laser frequency. Units in radians/sec.
- J. Number of velocity steps in calculation.
- K. Start up/Quit/Restart number. 0 = Start up. 1 = Quit. 2 = Restart.
- L. Initial iteration number in time loop.
- M. Initial velocity for the force function. Units are m/sec.
- N. The spacing variable for printing the output.
- O. Einstein A coefficient. Units of inverse seconds.
- P. Frequency of laser. Units of radians/sec.
- Q. The time increments that have data printed for them.

Figure 17. Data Input Format for  
FPLK Program

appendix is the modified form of the program. The changes amount to removing all constants which are inside the time loop in the program and calculating them outside the time loop. This saves amny calculations and speeds the program up by 20%. The program listed has been run for several different cases discussed in the thesis and yields the same answers.

Figure 18 is an example of the output format of the program. The velocity is printed along with the value of the distribution function and the force at that velocity. This is accomplished for all velocities for one time step. The computer then prints the number TOTNUM (the area under the distribution function), and then starts the calculations for the next time increment. Only six values of time are printed in the output file since it becomes quite large. The file wrtdat1 is used to take values from the program for these six times and input them into a graphics package. This package produces figures similar to those used in this thesis. The values in wrtdat1 are not labled as the values of outputx are. The first column in wrtdat1 is the velocity. The second column is the value of the distribution function at that velocity. The third is the force at that velocity and the fourth is the value of the time increment.

The size of the files wrtdat1 and outputx can become quite large for values of small velocity step size. For a velocity step size of .325 m/sec, the outputx file is

```

TIME= .479999988e-03
VELOCITY= -.200000000e+03 DFTN= .000000000e+00 FORCE= -.798820558e-22
VELOCITY= -.199625000e+03 DFTN= .000000000e+00 FORCE= -.799420029e-22
VELOCITY= -.199250000e+03 DFTN= .000000000e+00 FORCE= -.800020132e-22
VELOCITY= -.198875000e+03 DFTN= .000000000e+00 FORCE= -.800620991e-22
VELOCITY= -.198500000e+03 DFTN= .000000000e+00 FORCE= -.801222419e-22
VELOCITY= -.198125000e+03 DFTN= .000000000e+00 FORCE= -.801824604e-22
VELOCITY= -.197750000e+03 DFTN= .000000000e+00 FORCE= -.802427483e-22
VELOCITY= -.197375000e+03 DFTN= .000000000e+00 FORCE= -.803031056e-22
VELOCITY= -.197000000e+03 DFTN= .000000000e+00 FORCE= -.803635323e-22
VELOCITY= -.196625000e+03 DFTN= .000000000e+00 FORCE= -.804240285e-22
VELOCITY= -.196250000e+03 DFTN= .000000000e+00 FORCE= -.804845941e-22
VELOCITY= -.195875000e+03 DFTN= .000000000e+00 FORCE= -.805452291e-22
VELOCITY= -.195500000e+03 DFTN= .000000000e+00 FORCE= -.806059272e-22
VELOCITY= -.195125000e+03 DFTN= .000000000e+00 FORCE= -.806667074e-22
VELOCITY= -.194750000e+03 DFTN= .000000000e+00 FORCE= -.807275443e-22
VELOCITY= -.194375000e+03 DFTN= .000000000e+00 FORCE= -.807884570e-22
VELOCITY= -.194000000e+03 DFTN= .000000000e+00 FORCE= -.808494391e-22
VELOCITY= -.193625000e+03 DFTN= .000000000e+00 FORCE= -.809104906e-22
Vhb88H1183%193250000e+03 DFTN= .000000000e+00 FORCE= -.809716116e-22
VELOCITY= -.192875000e+03 DFTN= .000000000e+00 FORCE= -.810328019e-22
VELOCITY= -.192500000e+03 DFTN= .000000000e+00 FORCE= -.810940617e-22
VELOCITY= -.192125000e+03 DFTN= .000000000e+00 FORCE= -.811553972e-22
VELOCITY= -.191750000e+03 DFTN= .000000000e+00 FORCE= -.812167958e-22
VELOCITY= -.191375000e+03 DFTN= .000000000e+00 FORCE= -.812782702e-22
VELOCITY= -.191000000e+03 DFTN= .000000000e+00 FORCE= -.813398140e-22
VELOCITY= -.190625000e+03 DFTN= .000000000e+00 FORCE= -.814014209e-22
VELOCITY= -.190250000e+03 DFTN= .000000000e+00 FORCE= -.814631035e-22
VELOCITY= -.189875000e+03 DFTN= .000000000e+00 FORCE= -.815248618e-22
VELOCITY= -.189500000e+03 DFTN= .000000000e+00 FORCE= -.815866896e-22
VELOCITY= -.189125000e+03 DFTN= .000000000e+00 FORCE= -.816485804e-22
VELOCITY= -.188750000e+03 DFTN= .000000000e+00 FORCE= -.817105470e-22
VELOCITY= -.188375000e+03 DFTN= .000000000e+00 FORCE= -.817725831e-22
VELOCITY= -.188000000e+03 DFTN= .000000000e+00 FORCE= -.818346885e-22

```

Figure 18. Data Output Format for  
FPLK Program

two megabytes. The wrtdat1 file is 30% smaller for this case. This assumes that all the values calculated are written into the file. The use of the variable DFS in the input data allows only every Ith value of the velocity to be printed into the outputx and wrtdat1 files. Here I is the value assigned to the variable DFS. This can substantially reduce the size of the file. However, this will rule out being able to find the FWHM of the peak of the distribution function as it slows down. This is because the FWHM becomes very small and printing every Ith value of velocity will skip over the entire peak. If the FWHM is not desired, then the value for DFS can be set to allow a point every 20 m/sec to be printed and decent graphs will be produced.

The graphics package used to create the figures is called S (Ref 27). The values in wrtdat1 are read into a matrix in the S library. They are split into four vectors called force,df (value of the distribution function), vec (value of the velocity), and timex (value of the time increment the calculation is performed for). The figures generated for this thesis are plots of df versus vec. Thus, this is a graph of the distribution function for time J as a function of velocity. Figure 19 shows the program used to plot the distribution function. The plotter used is a HP 7220A plotter. It can be used interactively with the S package.

```
md_matrix(read('wrtdat22'),ncol=4,byrow=TRUE)
velctr_mdl[,1]
dftn_mdl[,2]
force_mdl[,3]
timex_mdl[,4]
vec22_split(velctr,timex)
df22_split(dftn,timex)
```

Figure 19. Graphics Program

The program in figure 19 can be executed from the shell of the Unix system. Unix is the operating system for the Vax computer. The execution statement is,

```
S BATCH odata pltdat
```

Here odata is the name of the program in figure 19 and pltdat is the name of a file that results and error messages will appear in when the program is executed. Note that S is a case sensitive language, and that the command S BATCH must be in capital letters. The ease of creating graphics programs in S, and the ability to execute them while in the Unix shell, outweighs the slow input/output times associated with the two software designs. The author found the combination of S and Unix to be a powerful one.

The program that plots the graphics has to be executed while in the S library. To enter S, type S while in the Unix system. To exit S type q . This command will automatically save all files created while in S and return the user to the Unix shell. An on line documentation for S is available by typing help while in the S library. A complete description of the plotting routines is given in the manual for the S package (Ref 27 pg 2-16).



```

hp7220h
par(oma=c(4,3,5,1))
par(mar=c(5,4,3,3))
mtext(side=1,line=1,cex=1.2,outer=TRUE,
      'Figure 16. Final Distribution for 480 MHz\nAccelerated Scan')
plot(vec22$[6],df22$[6],type='l')
box(1)
title ('','TIME= .48 millisec.','Velocity (m/sec)','Atomic
      Distribution Function (arbitrary units)')

```

Figure 20. Plotting Program

C THIS PROGRAM CALCULATES THE EFFECT OF A LASER ON AN ATOMIC  
C BEAM. IT IS A DIFFERENCE EQUATION OF THE FOKKER PLANCK EQUATION  
C DEVELOPED FOR THIS CASE BY M G MCHARG

```
REAL FORCE(20000),DFTN(20000),DELDFN(200000),MASS
REAL DELTIM,DELV,TOTNUM,OMEGAC,VEL(20000),ALPHA,TEMP,A
REAL VELO,VELMIN,PRENUM,TIME,WK,R,VELCTR(20000),FPRIME(20000)
REAL DIFUSN(20000),DEFCTV(20000),PFTN(20000),DPRIME(20000)
INTEGER DFS,MT,N,Q,JCNTR
```

C THIS SECTION OPENS THE FILES wrtdata1 AND save. wrtdata1 IS THE FILE FOR  
C DATA TO BE INPUTED INTO THE GRAPHICS. save IS A FILE THAT SAVES THE  
C VALUE FOR JCNTR AND THE VECTORS VELCTR DFTN FORCE AND DIFUSN.

```
OPEN(10,FILE='wrtdata1')
REWIND 10
OPEN(11,FILE='save')
REWIND 11
```

```
PRINT*,"VARIABLE LIST"
PRINT*,"FORCE: 2400 ELEMENT VECTOR. FORCE DISTRIBUTION FTN"
PRINT*,"DFTN: 2400 ELEMENT VECTOR. DISTRIBUTION FTN TO BE"
PRINT*,"      USED IN BOLTZMAN EQTN."
PRINT*,"MASS: PARTICLE MASS,KILOGRAMS"
PRINT*,"DELTIM: INCREMENT OF TIME IN DIFFERENCING EQTN."
PRINT*,"DELV: CHANGE IN VELOCITY IN DIFFERENCING EQTN."
PRINT*,"TOTNUM: THE AREA UNDER THE DFTN CURVE."
PRINT*,"VELCTR: VELOCITY "
PRINT*,"ALPHA: WIDTH OF DFTN IN METERS PER SECOND"
PRINT*,"TEMP:TEMPERATURE IN DEGREES KELVIN OF OVEN PRODUCING THE"
PRINT*,"      ATOMS"
PRINT*,"A: SPONTANEOUS EMISSION COEFFICIENT, INVERSE SECONDS"
PRINT*,"OMEGAC: CAPITAL OMEGA, RABI FREQUENCY,INVERSE SECONDS"
PRINT*,"VELMIN: MINIMUM VELOCITY IN DFTN."
PRINT*,"VELO: THE INITIAL VELOCITY WHICH FORCE AFFECTS "
PRINT*,"TIME: A CONSTANT USED TO TELL INTERACTION TIME"
PRINT*,"DFS: SPACING INTEGER FOR OUTPUT PRINTING "
PRINT*,"PRENUM: THE PRELIMINARY TOTNUM"
PRINT*,"MT: TOTAL NUMBER OF TIME ITERATIONS THE PROGRAM RUNS"
PRINT*,"R:RATE LASER FREQ IS SWEEP, IN INVERSE SECONDS"
PRINT*,"      SQUARED"
PRINT*,"DETUNF: THE DUTUNING FREQUENCY BETWEEN LASER AND"
PRINT*,"      THE ABSORBING LINE OF THE MEDIA"
PRINT*,"WK: WAVENUMBER. 2*PI/LAMBDA IN INVERSE METERS"
PRINT*,"LAMBDA: THE WAVELENGTH OF THE LASER IN METERS"
PRINT*,"DELFTN: THE CHANGE IN THE DFTN"
PRINT*,"N: THE END NUMBER IN DO LOOPS"
PRINT*,"KBOLT: BOLTSMAN CONSTANT IN JOULES PER DEGREE KELVIN"
PRINT*,"DIFUSN:20000 ELEMENT VECTOR,DIFUSION COEFFICIENT "
PRINT*,"DEFCTV:20000 ELEMENT VECTOR,DEFEFFECTIVE "
```

```

PRINT*, "W THE FREQUENCY OF LASER IN INVERSE SECONDS(RADIAN)"
PRINT*, "SPDLIT: THE SPEED OF LIGHT IN MKS"
PRINT*, "DELTIM: TIME STEP SIZE IN SECONDS"
PRINT*, "DELV: VELOCITY STEP SIZE IN METERS PER SECOND"
PRINT*, "QUIT: A COUNTER SET EQUAL TO 0,1,2 FOR START,END,RESTART"
PRINT*, "      RESPECTIVELY"
PRINT*, "JCNTR: VALUE FOR THE TIME DO LOOP. SET IT EQUAL TO 1 IF"
PRINT*, "      FIRST START,SET EQUAL TO LAST VALUE OF J IF RESTART"
PRINT*, "B,G,D,E,F: VALUES OF TIME COUNTER AT WHICH THE PROGRAM"
PRINT*, "      PRINTS THE OUTPUT VALUES"
PRINT*, "HBAR: PLANCKS CONTANT DIVIDED BY 2*PI,JOULES-SECONDS"
PRINT*, "C: MOMENTUM OF PHOTONS IN KILOGRAM-METERS PER SECOND"
PRINT*, "Q: COUNTER OF THE TIME INCREMENTS. WHEN IT REACHES 100"
PRINT*, "      VALUE FOR JCNTR AND THE VECTORS VELCTR,DFTN,FORCE"
PRINT*, "      AND DIFUSN ARE SAVED IN THE SAVE FILE"

```

```

PRINT*, " "

```

```

C   THIS SECTION READS IN INITIAL VALUES
PRINT*, "INPUT MASS,DELTIM,DELV,VELMIN,OMEGAC,TEMP,WK,MT,R,N"
READ*, MASS,DELTIM,DELV,VELMIN,OMEGAC,TEMP,WK,MT,R,N
PRINT*, "MASS=",MASS,"DELTIM=",DELTIM,"DELV=",DELV
PRINT*, "VELMIN=",VELMIN,"OMEGAC=",OMEGAC,"TEMP=",TEMP
PRINT*, "WK=",WK,"MT=",MT,"R=",R,"N=",N
PRINT*, "INPUT QUIT AND JCNTR"
READ*, QUIT,JCNTR
PRINT*, "QUIT=",QUIT,"JCNTR=",JCNTR
PRINT*, "INPUT VELO","INPUT DFS","INPUT A"
READ*, VELO,DFS,A,W
PRINT*, "VELO=",VELO,"DFS=",DFS,"A=",A,"W=",W
READ*, B,G,D,E,F
PRINT*, "B=",B,"G=",G,"D=",D,"E=",E,"F=",F

```

```

C   QUIT IS THE START/QUIT/RESTART OPTION. IF QUIT=1 THEN PROGRAM ENDS
C   IF QUIT=2 THEN PROGRAM RESTARTS,IF QUIT=0 THEN PROGRAM STARTS FOR
C   FIRST TIME.

```

```

IF (QUIT .EQ. 1) THEN
  GO TO 92
END IF
IF (QUIT .EQ. 2) THEN
  READ(11,*)JCNTR
  DO 40 I=1,N
    READ(11,*)VELCTR(I),DFTN(I),FORCE(I),DIFUSN(I)
40  CONTINUE
  REWIND 11
  GO TO 82
END IF

```

```

C   THIS DO LOOP INITIALIZES THE VELOCITY DISTRIBUTION FTM
BOLTK=1.38E-23
ALPHA=SQRT(2.*TEMP*BOLTK/MASS)
DO 50 I=1,N
  VEL(I)=DELV*(I-1)-VELMIN
  IF(VEL(I).LT.0) THEN
    VEL(I)=0

```

```

  END IF

```

```

C      THE VELCTR SERVES TO PRINT THE REAL VELOCITY AXIS
      VELCTR(I)=DELV*(I-1)-VELMIN
      DEFCTV(I)=- (WK*VELO)+WK*VELCTR(I)
      DFTN(I)=((VEL(I)**3)/(ALPHA**4))*EXP(-(VEL(I)**2)/(ALPHA**2))
50    CONTINUE
      PRINT*, " "
      C=WK*1.0546E-34
      HBAR=1.054E-34
      SPDLIT=2.998E8
C      THE DO 70 LOOP CALCULATES THE TOTAL NUMBER TOTNUM

      PRINT*, " "
C      THE FOLLOWING ARE CONSTANTS USED IN THE CALCULATIONS OF FORCE
C      AND DIFUSN.

      W=SPDLIT*WK
      DIFCO1=HBAR*W*OMEGAC/MASS
      DIFCO=(DIFCO1/SPDLIT)*(DIFCO1/SPDLIT)*(A/5.)
      DIFC1=A*A+2.*OMEGAC*OMEGAC
      DIFC2=-A*A+2.*OMEGAC*OMEGAC
      DIFC3=2.*OMEGAC*OMEGAC*A*HBAR
      DIFC4=OMEGAC*OMEGAC*WK*WK*HBAR/2.
      DELDC1=DELTIM/DELV/DELV
      CINT1=(DELV-(DELTIM*R/WK))
      DELDC2=(-DELTIM/(MASS*DELV))

C      THE DO 86 LOOP MAKES THE DIFFUSION COEFFICIENT SO THE DELDFN
C      CAN BE COMPUTED.
      DO 86 I=1,N
      DIFUSN(I)=(DIFC4*(DIFC3*(12.*DEFCTV(I)+DIFC2)+A*(4.*DEFCTV(I)*
C      DEFCTV(I)+A*A)*HBAR*(4.*DEFCTV(I)*DEFCTV(I)+A*A))/(MASS*(4.*
C      DEFCTV(I)*DEFCTV(I)+DIFC1))/(MASS*(4.*DEFCTV(I)*DEFCTV(I)+
C      DIFC1))/(4.*DEFCTV(I)*DEFCTV(I)+DIFC1))+DIFCO/(4.*DEFCTV(I)*
C      DEFCTV(I)+DIFC1)
86    CONTINUE
C      THE DO 85 LOOP MAKES THE FORCE COEFFICIENTS SO THE DO 90 LOOP
C      CAN STEP OUT IN TIME.
      DO 85 I=1,N
      FORCE(I)=- (A*OMEGAC*C*OMEGAC)/(4.*DEFCTV(I)*DEFCTV(I)+A*A+
C      2*OMEGAC*OMEGAC)
85    CONTINUE
C      THE DO 87 LOOP PRINTS THE INITIAL VALUES OF EVERYTHING
      PRINT*, "TIME=0"
      DO 87 I=1,N,DFS
      PFTN(I)=DFTN(I)*100.
      PRINT*, "VEL=", VELCTR(I), "DFTN=", PFTN(I), "FORCE=", FORCE(I)
      WRITE(10,990)VELCTR(I),PFTN(I),FORCE(I),J
990    FORMAT(5X,E12.5,2X,E12.5,2X,E12.5,2X,I5)
87    CONTINUE
      TOTNUM=0
      DO 70 I=1,N
      PRENUM=0
      PRENUM=DELV*DFTN(I)
      TOTNUM=TOTNUM+PRENUM
70    CONTINUE
      PRINT*, "TOTNUM=", TOTNUM

```

```

PRINT*, ' '
PRINT*, ' '
Q=0

```

```

C      THIS IS THE TIME LOOP. IT CALCULATES VALUES FOR THE JTH
C      ITERATION USING VALUES FROM THE J-1TH ITERATION
82     DO 90 J=JCNTR,MT
        TIME=J*DELTIM

C      THE DO 91 LOOP INTERPOLATES TO MOVE THE FORCE AND DIFFUSION
C      COEFFICIENTS DOWN THE VELOCITY AXIS. THIS KEEPS THE PROGRAM
C      FROM RECALCULATING THE COEFFICIENTS EACH TIME.
        DO 91 I=1,N-1
            DPRIME(I)=- (CINT1*(DIFUSN(I+1)-DIFUSN(I))/DELV)+DIFUSN(I+1)
            FPRIME(I)=- (CINT1*(FORCE(I+1)-FORCE(I))/DELV)+FORCE(I+1)
91     CONTINUE

C      THE DO 100 LOOP FINISHES MOVING THE FORCE AND DIFFUSION
C      COEFFICIENTS DOWN THE VELOCITY AXIS.
        DO 100 I=1,N
            DIFUSN(I)=DPRIME(I)
            FORCE(I)=FPRIME(I)
100    CONTINUE

C      THE DO 80 LOOP CHANGES THE DISTRIBUTION FTN FOR VELOCITY
        DO 80 I=2,N-1
            DELDFN(I)=DELD C2*(FORCE(I+1)*DFTN(I+1)
C      -FORCE(I)*DFTN(I))+ (DELD C1*(DIFUSN(I+1)*DFTN(I+1)-2.*
C      DIFUSN(I)*DFTN(I)+DIFUSN(I-1)*DFTN(I-1)))
80     CONTINUE

C      THE DO 81 LOOP CHANGES THE DISTRIBUTION FUNCTION FOR VELOCITY
        DO 81 I=1,N
            DFTN(I)=DFTN(I)+DELD F(I)
81     CONTINUE

C      THE DO 75 LOOP PRINTS THE VELOCITY,DFTN,FORCE.
        IF (J.EQ.B.OR.J.EQ.G.OR.J.EQ.D.OR.J.EQ.E.OR.J.EQ.F) THEN
            PRINT*, 'TIME=', TIME
            DO 75 I=1,N,DFS
                PFTN(I)=DFTN(I)*100
                PRINT*, 'VELOCITY=', VELCTR(I), 'DFTN=', PFTN(I), 'FORCE=', FORCE(I)
                WRITE(10,1000) VELCTR(I), PFTN(I), FORCE(I), J
1000    FORMAT(5X,E12.5,2X,E12.5,2X,E12.5,2X,I5)
75     CONTINUE
            PRINT*, 'TOTNUM=', TOTNUM
            END IF

C      THE DO 76 LOOP RECALCULATES TOTNUM
            TOTNUM=0
            DO 76 L=1,N
                PRENUM=0
                PRENUM=DELV*DFTN(L)
                TOTNUM=TOTNUM+PRENUM
76     CONTINUE

```

```

      JCNTR=J
C     THE Q COUNTER PRINTS EVERY 100 TIME AND TOTNUM
      Q=Q+1
      IF(Q.EQ.100)THEN
      Q=0
      WRITE(11,*)JCNTR
      DO 77 I=1,N
      WRITE(11,*)VELCTR(I),DFTN(I),FORCE(I),DIFUSN(I)
77    CONTINUE
      REWIND 11

```

```

PRINT*, 'TIME=', TIME
PRINT*, ' '
PRINT*, 'TOTNUM=', TOTNUM

```

```

PRINT*, ' '
PRINT*, ' '
PRINT*, ' '
END IF
90    CONTINUE
92    END
X

```

## VITA

Matthew G. McHarg was born 1 May 1957 in Knoxville, Tennessee. He graduated from high school in Joplin Missouri. In 1979, he graduated from Missouri Souther State College with a Bachelor of Science degree in Physics. He graduated from Air Force Officers Training School on 6 June 1980. Subsequently, he was assigned to the Foreign Technology Division at Wright Patterson Air Force Base. In 1982, he entered the Air Force Institute of Technology in the Engineering Physics Department.

Permanent Address: 4920 S. Pennsylvania  
Englewood, CO. 80110

AD-A163 954  
REPORT DOCUMENTATION PAGE

1a. REPORT SECURITY CLASSIFICATION Unclassified		1b. RESTRICTIVE MARKINGS None	
2a. SECURITY CLASSIFICATION AUTHORITY		3. DISTRIBUTION/AVAILABILITY OF REPORT Approved for public release; distribution unlimited	
2b. DECLASSIFICATION/DOWNGRADING SCHEDULE			
4. PERFORMING ORGANIZATION REPORT NUMBER(S) AFIT/GER/PH/83D-6		5. MONITORING ORGANIZATION REPORT NUMBER(S)	
6a. NAME OF PERFORMING ORGANIZATION School of Engineering Air Force Institute of Tech.	6b. OFFICE SYMBOL (If applicable) AFIT/EN	7a. NAME OF MONITORING ORGANIZATION	
6c. ADDRESS (City, State and ZIP Code) Wright-Patterson AFB Ohio 45433		7b. ADDRESS (City, State and ZIP Code)	
8a. NAME OF FUNDING/SPONSORING ORGANIZATION	8b. OFFICE SYMBOL (If applicable)	9. PROCUREMENT INSTRUMENT IDENTIFICATION NUMBER	
8c. ADDRESS (City, State and ZIP Code)		10. SOURCE OF FUNDING NOS.	
		PROGRAM ELEMENT NO.	PROJECT NO.
		TASK NO.	WORK UNIT NO.
11. TITLE (Include Security Classification) LASER COOLING OF NEUTRAL ATOMS			
12. PERSONAL AUTHOR(S) Matthew G. Mc Harg 1st Lt Air Force			
13a. TYPE OF REPORT MS Thesis	13b. TIME COVERED FROM TO	14. DATE OF REPORT (Yr., Mo., Day) 1983 December	15. PAGE COUNT 115
16. SUPPLEMENTARY NOTATION			
17. COSATI CODES		18. SUBJECT TERMS (Continue on reverse if necessary and identify by block number)	
FIELD	GROUP	SUB. GR.	
19. ABSTRACT (Continue on reverse if necessary and identify by block number)  Thesis advisor: Major Richard J. Cook  <div style="text-align: right;"><i>Approved for public release: IAW AFR 120-4.</i> <i>John E. Wolaver</i> 16 JAN 86 Dean for Research and Professional Development Air Force Institute of Technology (AFIT) Wright-Patterson AFB OH 45433</div>			
20. DISTRIBUTION/AVAILABILITY OF ABSTRACT Unclassified/UNLIMITED <input checked="" type="checkbox"/> SAME AS RPT. <input type="checkbox"/> DTIC USERS <input type="checkbox"/>		21. ABSTRACT SECURITY CLASSIFICATION Unclassified	
22a. NAME OF RESPONSIBLE INDIVIDUAL Major Richard J. Cook PhD		22b. TELEPHONE NUMBER (Include Area Code) (513)-255-5187	22c. OFFICE SYMBOL AFIT/ENP



Abstract

The theory of the resonance radiation force is studied as it applies to the slowing of a two-level atom using a swept frequency laser. The theory is developed in detail for this case. A single partial differential equation called the Fokker-Planck equation is found to describe the atomic motion for many cases. This equation is solved numerically for a one dimensional geometry. Results from this numerical solution are found to be within 10% of experimental results. Analysis of this problem in one dimension leads to the prediction that for fixed amounts of frequency sweeping, a faster scan rate will yield smaller full width at half maximum (FWHM) spread in the velocity distribution for the atomic beam. This program also predicts that the atoms can be slowed arbitrarily close to 0 m/sec using this technique. The program used for this analysis is included.

*no data to file 8*

**END**

**FILMED**

3-86

**DTIC**